

THE DEMOCRATIC AND POPULAR REPUBLIC OF ALGERIA
MINISTRY OF HIGHER EDUCATION AND
SCIENTIFIC RESEARCH
UNIVERSITY SAAD DAHLEB BLIDA - 1



INSTITUTE OF AERONAUTICS AND SPACE STUDIES
DEPARTEMENT OF SPACE STUDIES

Final year Dissertation
For The Purpose of obtaining
MASTER's Degree in Aeronautics
OPTION: TELECOMMUNICATIONS SPATIALES

THEME

**Performance Analysis of LoRa Modulation
For CubeSat Communication Subsystem**

Presented by:

- ABBOURA Ibrahim Abderrahmen
- AMROUCHE Amazigh

Board of Examiners:

- | | | |
|------------------------|------------|------|
| • Dr. Lila MOUFFOK | President | IAES |
| • Dr. Ahmed MOUMENA | Examiner | IAES |
| • Dr. Sofiane TAHRAOUI | Supervisor | IAES |

Academic year 2023/2024

ABSTRACT

This study examines the use of LoRa modulation in the communication systems of CubeSats, a prominent type of nano-satellite. We explore the evolution of spacecraft miniaturization, emphasizing the benefits of nano-satellites, such as reduced costs and shorter development cycles. CubeSats, with their modular design and use of off-the-shelf components, offer a cost-effective and efficient solution for space missions. However, communication challenges persist due to their small size. Through MATLAB simulations and PCB design with EasyEDA, we analyze the performance of LoRa modulation in enhancing CubeSat communication. This research aims to advance the understanding and implementation of efficient communication systems in CubeSat technology.

KEY WORDS: CubeSat, Lora Modulation, Nano-satellites.

RESUME

Cette étude examine l'utilisation de la modulation LoRa dans les systèmes de communication des CubeSats, un type de nano-satellite. Nous explorons l'évolution de la miniaturisation des engins spatiaux en mettant l'accent sur les avantages des nano-satellites, tels que la réduction des coûts et des cycles de développement plus courts. Les CubeSats, avec leur conception modulaire et l'utilisation de composants disponibles dans le commerce, offrent une solution économique et efficace pour les missions spatiales. Cependant, des défis de communication persistent en raison de leur petite taille. À travers des simulations MATLAB et la conception de PCB avec EasyEDA, nous analysons la performance de la modulation LoRa pour améliorer la communication des CubeSats. Cette recherche vise à améliorer la compréhension et la mise en œuvre des systèmes de communication efficaces dans la technologie CubeSat.

ملخص

تدرس هذه الدراسة استخدام تعديل LoRa في أنظمة الاتصالات الخاصة بـ CubeSats، وهو نوع بارز من الأقمار الصناعية النانوية. نستكشف تطور تصغير المركبات الفضائية، مع التركيز على فوائد الأقمار الصناعية النانوية، مثل انخفاض التكاليف ودورات التطوير الأقصر. نقدم CubeSats، بتصميمها المعياري واستخدامها لمكونات جاهزة، حلاً فعالاً من حيث التكلفة والكفاءة للمهام الفضائية. ومع ذلك، لا تزال تحديات الاتصال قائمة بسبب صغر حجمها. من خلال محاكاة MATLAB وتصميم PCB باستخدام EasyEDA، نقوم بتحليل أداء تعديل LoRa في تحسين اتصالات CubeSat. يهدف هذا البحث إلى تعزيز فهم وتنفيذ أنظمة الاتصالات الفعالة في تكنولوجيا CubeSat.

ACKNOWLEDGMENT

I would like to express my heartfelt gratitude to my supervisor, **Dr. Sofiane TAHRAOUI**, for their continuous support, guidance, and encouragement throughout this research.

I am also grateful to my examiner, **Dr. Ahmed MOUMENA**, and the president of the examination committee, **Dr. Lila MOUFFOK**, for their valuable feedback and insights.

A special thank you to my professors, **Mr. Salim DJEZZAR**, **Ms. Houria AZINE** for their inspiration and mentorship.

I extend my sincere thanks to the company **ST Engineering** for their support and collaboration, which were essential for this work.

Lastly, I thank my family and friends for their unwavering support and encouragement.

Thank you all.

DEDICATION

I dedicate this work to my precious and lovely family, my father and my mother, my sister and my brother ISLAM (اللهم ارحمه), the source of my hope, my inspiration, my strength and my happiness in life.

A special dedicate to all the family ABBOURA, and ABDENNOUR.

To my friends ABDELKRIM, ZEYD, HEYTHEM, MOHAMMED and ABDELHAK.

I also would like to dedicate this thesis to BOUALEM, MAHDI, AMAZIGH, ABDEL-KADER and LYDIA the first persons I met during my years at university.

IBRAHIM

Special thanks to my beloved parents, Yassine and Cherifa, for their unwavering support and belief in me, and to my brothers, Ilian, Chemsou, and Chihab, and my sister, Anfel, for their endless love and encouragement. My precious family, thank you for always being there for me.

A special dedicate To all the family AMROUCHE, and HAMI.

I also dedicate this thesis to Boualem, Ibrahim, Mahdi, and Abdel-Kader. Your friendship and companionship have made my university years unforgettable.

Amazigh

A special dedicate to our second family who was there for me all over the five years (L7ou's Family).

TABLE OF CONTENT

ABSTRACT	1
RESUME.....	1
ملخص.....	1
AKNOWLEDGMENT.....	2
DEDICATION	3
TABLE OF CONTENT	4
LIST OF FIGURES.....	7
LIST OF TABLES.....	8
Abbreviation List.....	9
GENERAL INTRODUCTION	10
CHAPTER I Introduction To Nanosatellite (CubeSat).....	12
I.1 Introduction.....	12
I.2 Mass Categories	12
I.3 Satellite size vs cost and applications	13
I.4 The Evolution of Small Satellite Launches by Weight Class (2010-2022).....	14
I.5 The Rise of CubeSats: Democratization and the Accessibility of Space.....	15
I.6 CubeSat Application.....	15
I.7 Satellite Subsystems.....	16
I.8 Communication Sub-system	16
I.8.1 Transmitter/Receivers.....	17
I.8.2 Antenna.....	17
I.9 Conclusion	19
CHAPTER II Introduction to CubeSat Communication System.....	20
II.1 Introduction	20
II.2 Detailed study of the synoptic diagram for the communication Sub-system.....	21
II.2.1 Source	21
II.2.2 Coding (FEC).....	22
II.2.2.1 Example of the process in Forward Error Correction protocol	22
II.2.3 Bits to Symbols (Mapping)	22
II.2.4 LoRa Modulation	23
II.2.4.1 Why Lora modulation?.....	23
II.2.4.2 Overview of the CSS modulation.....	23
II.2.4.3 LoRa Spread Spectrum	23

II.2.4.4 Mathematical Equation for The SIGNAL $T(n)$	24
II.2.4.5 Impact of Spreading Factor (SF) on LoRa Communication.....	25
II.2.4.5.1 Range	26
II.2.4.5.2 The data rate	26
II.2.4.5.3 Noise resilience.....	27
II.2.4.6 Up-Chirp and Down-Chirp Signals	27
II.2.4.6.1 Characteristics of Up-Chirp	28
II.2.4.6.2 Comparison with Down-Chirp.....	28
II.2.4.7 Lora modulation coding.....	28
II.2.4.8 LoRa modulation characteristics.....	29
II.2.4.9 LoRa physical layer.....	31
II.2.4.10 LoRa Link Budget	32
II.2.4.11 Comparative Analysis of FSK and LoRa	32
II.2.4.11.1 Range	33
II.2.4.11.2 Sensitivity.....	33
II.2.4.11.3 Data Rate	34
II.2.4.12 Power Consumption and Sleep Mode in LoRa Modules for CubeSat Systems	34
II.2.4.12.1 Overview of Power Consumption.....	34
Sleep Mode in LoRa Modulation.....	35
II.2.4.12.2 How Sleep Mode Works in LoRa Modulation.....	36
II.2.5 Introduction to Software Defined Radio (SDR) and its Integration in CubeSat Communication Systems.....	37
II.2.5.1 LimeSDR Mini.....	38
II.2.5.2 HackRF One	38
II.2.6 Channel	39
II.2.7 LoRa Demodulation	39
II.2.8 Symbols to Bits:	39
II.2.9 Decoding.....	40
II.2.10 Sink.....	40
II.3 Conclusion.....	40
CHAPTER III Simulation and Performance Evaluation of LoRa.....	41
III.1 Introduction.....	41
III.2 LoRa performance with deferent Spreading Factors.....	41
Block A: Initialization.....	42

Block B: Generate LoRa Symbol	42
Block C: Add Noise and Demodulate	42
Block D: Plot Histogram and Calculate SER	43
III.3 Simulation Results	43
III.4 Simulation Discussion	46
III.4.1 Impact of SNR on Error Rate	46
III.4.1.1 Trade-off between Spreading Factor, Range, and Data Rate	47
III.4.1.1.1 Higher Spreading Factor (SF = 12)	47
III.4.1.1.2 Lower Spreading Factor (SF = 7)	47
III.4.1.1.3 Intermediate Spreading Factor (SF = 9)	47
III.5 Simulation Conclusion	47
III.6 Designing the Communication System: Component Selection and PCB Layout	48
III.6.1 Component Selection for the Communication System	49
III.6.1.1 SX1280 Transceiver	49
III.6.1.2 Arduino Nano	49
III.6.1.3 Sensors	50
III.6.1.3.1 ICM 20948 Module	50
III.6.1.3.2 NEO-6M GPS Module	51
III.6.1.3.3 DHT 11 Module	51
III.6.1.4 Antenna	52
III.7 CubeSat Communication System: Schematic and PCB Blueprint	53
III.8 PCB design	55
III.9 Conclusion	56
General Conclusion	57
References	58

LIST OF FIGURES

FIGURE 1 : SATELLITE APPLICATIONS.	12
FIGURE 2 : MASS CATEGORIES OF SATELLITES	13
FIGURE 3 : LAUNCHES OF SMALL SATELLITES (1~400KG) (SUCCESSFUL LAUNCHES ONLY)	14
FIGURE 4 : SATELLITE SUBSYSTEMS	16
FIGURE 5: BASIC COMMUNICATION SUBSYSTEM SCHEME.....	17
FIGURE 6 : LOW FREQUENCY / LONG WAVELENGTH	18
FIGURE 7 : HIGH FREQUENCY / SHORT WAVELENGTH	18
FIGURE 8: YAGI-ANTENNA FOR VHF-BAND	18
FIGURE 9: DISH-ANTENNA FOR S-BAND.....	18
FIGURE 10 : COMMUNICATION CHANNEL.....	20
FIGURE 11: DETAILED SYNOPTIC DIAGRAM FOR RECENT COMMUNICATION SUBSYSTEM.....	21
FIGURE 12: FEC (FORWARD ERROR CORRECTION) CHANNEL.....	22
FIGURE 13: CHIRP PROPAGATION WAVE	24
FIGURE 14 : COMPARISON OF THE LORA SPREADING FACTORS SF=7 TO SF=12	25
FIGURE 15 : GRAPH ILLUSTRATES THE IMPACT OF THE SPREADING FACTOR (SF) ON RANGE, DATA RATE, AND NOISE RESILIENCE IN LORA COMMUNICATION	26
FIGURE 16 : UP CHIRP SIGNAL	28
FIGURE 17 : DOWN CHIRP SIGNAL	28
FIGURE 18 : CHIRP SPREAD SPECTRUM CODING PROCESS	29
FIGURE 19 : LORA PHYSICAL FRAME.....	31
FIGURE 20 : POWER CONSUMPTION COMPARISON WITHOUT SLEEP MODE VS WITH SLEEP MODE.	35
FIGURE 21: SLEEP MODE PRINCIPLE.....	36
FIGURE 22 : LIMESDR MINI	38
FIGURE 23 : HACKRF ONE.....	39
FIGURE 24 : MATLAB CODE ORGANIGRAMME.	41
FIGURE 25 : SER FOR SF =7 AND SNR = -10.	43
FIGURE 26 : SER FOR SF =7 AND SNR = -15.	43
FIGURE 27 : FIGURE 27 SER FOR SF =9 AND SNR = -15.....	44
FIGURE 28 SER FOR SF =9 AND SNR = -5.....	44
FIGURE 29 : FIGURE 27 SER FOR SF =9 AND SNR = -28.....	44
FIGURE 30 : FIGURE 27 SER FOR SF =12 AND SNR = -10.....	45
FIGURE 31 : FIGURE 27 SER FOR SF =9 AND SNR = -25.....	45
FIGURE 32 : FIGURE 27 SER FOR SF =9 AND SNR = -30.....	45
FIGURE 33 : IMPACT OF SNR ON ERROR RATE.....	46
FIGURE 34 : FUNDAMENTAL COMMUNICATION SYSTEM FOR AN EDUCATIONAL CUBESAT.	48
FIGURE 35 : SX1280 TRANSCEIVER	49
FIGURE 36 : ARDUINO NANO MODULE.....	50
FIGURE 37 : ICM 20948 MODULE.	50
FIGURE 38 : NEO-6M GPS MODULE.....	51
FIGURE 39 : DHT 11 MODULE	51
FIGURE 40 : 2.4 GHZ DIPOLE ANTENNA WITH SMA CONNECTOR	52
FIGURE 41 : WIFI YAGI ANTENNA (2.4 GHZ).	52
FIGURE 42 : DESIGN SCHEMATIC FOR THE EMISSION PART	53
FIGURE 43 : DESIGN SCHEMATIC FOR THE RECEPTION PART.	54
FIGURE 45 PCB DESIGN SCHEMATIC FOR THE EMISSION PART.....	55
FIGURE 44 PCB DESIGN SCHEMATIC FOR THE RECEPTION PART	55

LIST OF TABLES

TABLE 1 : EVALUATING THE ADVANTAGES OF SMALL SATELLITES OVER BIG SATELLITES	14
TABLE 2 : LINK BUDGET COMPARISON LORA VS FSK	33
TABLE 3 : COMPARISON TABLE BETWEEN THE YAGI ANTENNA FROM AND THE TP-LINK DIPOLE ANTENNA	53

Abbreviation List

LoRa: Long Range.

IoT: Internet of Things.

M2M: Machine to Machine.

PCB: Printed Circuit Board.

VHF: Very High frequency.

CSS: Chirp Spread Spectrum.

TNC: Terminal Node Controller.

UHF: Ultra High Frequency.

FEC: Forward Error Correction.

SF: Spreading Factor.

FSK: Frequency Shift Keying.

CR: Code Rate.

BW: Bandwidth.

PHY: Physical Layer.

CRC: Cyclic Redundancy Check.

SNR: Signal-to-Noise Ratio.

SER: symbol error rate.

FFT: Fast Fourier Transform.

ER: Error Rate.

SDR: Software Defined Radio.

ADCS: Attitude Determination and Control System.

IMU: Inertial Measurement Unit.

CISO: CubeSat for Ionospheric Scattering Observations.

GENERAL INTRODUCTION

The evolution of spacecraft technology has been marked by significant advancements in miniaturization. Initially, spacecraft such as Sputnik 1, which weighed over 180 pounds, represented the pioneering era of space exploration. However, the advent of miniaturized electronics has given rise to nano-satellites, compact spacecraft ranging between 2 and 22 pounds. These nano-satellites offer substantial advantages: they are more cost-effective to build and launch, have shorter development cycles, and can be deployed in multiples to execute more complex missions. Consequently, nano-satellites are democratizing access to space and paving the way for innovative applications and missions.

CubeSats, a widely recognized and popular type of nano-satellite, present an intriguing avenue in satellite technology. These small, standardized satellites are constructed in modular units, each approximately the size of a Rubik's Cube. The use of off-the-shelf components renders CubeSats lightweight, cost-effective, and amenable to rapid development. Their affordability and compact size make them particularly well-suited for educational projects, technology demonstrations, and Earth observation missions. In these contexts, CubeSats can effectively gather data or conduct experiments in space, thereby broadening access to space and enabling a variety of scientific and technological advancements [1].

One of the key innovations that make CubeSats successful is their modularity, which significantly reduces development costs and time. However, CubeSats face communication challenges due to their small size. They require systems that prioritize miniaturization and low power consumption while maintaining adequate data transmission rates. This is where the transceiver, a space-borne radio for both transmitting and receiving data, is crucial. Paired with a directional antenna, the transceiver handles command uplinks from ground stations and telemetry downlinks, all within the CubeSat's strict size, weight, and power constraints [2].

When it comes to the radio communication systems of CubeSats, various forms of frequency or phase modulation are typically used. More sophisticated modulation methods can greatly enhance the efficiency of the radio link. One such method is LoRa modulation, which is commonly used in machine-to-machine (M2M) communications and IoT wireless sensor networks. LoRa modulation employs a spread-spectrum technique, encoding data with a wide-band chirp signal where the frequency linearly increases or decreases over time [1].

In our study, we will explore a communication system for a Nano-satellite (CubeSat) utilizing LoRa modulation. This involves several key steps. First, we will simulate the spread spectrum technique, along with the transmission and reception processes, using MATLAB to analyze the performance and efficiency of LoRa¹ modulation in this context. Additionally, we will design and implement a printed circuit board (PCB) for the communication system using EasyEDA software. This detailed design will include the integration of all necessary components to ensure effective communication for the CubeSat. As this is a first exploratory study in the domain of CubeSat technology and design, we aim to provide a comprehensive understanding of how LoRa modulation can be effectively implemented in CubeSat communication subsystems.

¹ LoRa (Long Range) modulation is a type of wireless communication technology specifically designed for low power, long-range, and low-data-rate applications. It is particularly well-suited for Internet of Things (IoT) devices, where battery life and range are critical factors.

I.1 Introduction

Satellites play a vital role in our daily lives, with various types contributing to our well-being. Earth observation satellites help with weather forecasting and environmental monitoring, while communication satellites enable global connectivity and access to information. Navigation satellites provide precise location and timing information, and scientific satellites aid in space research and astronomy. Military satellites support national security, and commercial satellites provide data transfer and services like satellite TV and internet access [1].

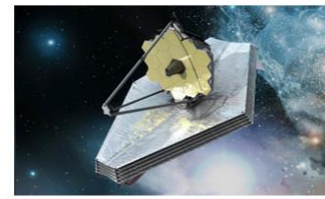
There are a wide range of satellite application which we benefit from [1].



a) Earth Observation using Satellite remote sensing



b) Intercontinental and Long-Distance Communication via Satellite (Satcom)



c) Deep space exploration Satellite (ex :james)

Figure 1 : Satellite Applications.

I.2 Mass Categories

The evolution of satellites has been marked by significant advancements in reducing their mass while increasing their capabilities. From the early days of massive satellites weighing up to 6 tons, we have come a long way. Today, we have Pico-satellites weighing just a few kilograms, micro-satellites weighing around 10-100 kilograms, Nano-satellites weighing around 1-10 kilograms, small satellites weighing around 10-100 kilograms, and medium satellites weighing around 100-500 kilograms. This reduction in mass has been made possible by advancements in technology, leading to more efficient and cost-effective satellite systems. For example, small satellites like CubeSats have become increasingly popular due to their low cost and high performance. They are used for a variety of applications, including Earth observation, communication, and scientific research. On the other hand, medium satellites are used for more complex missions, such as deep space exploration and interplanetary

communication. The reduction in mass has also led to an increase in the number of satellites being launched into space, making space more accessible and affordable [2].

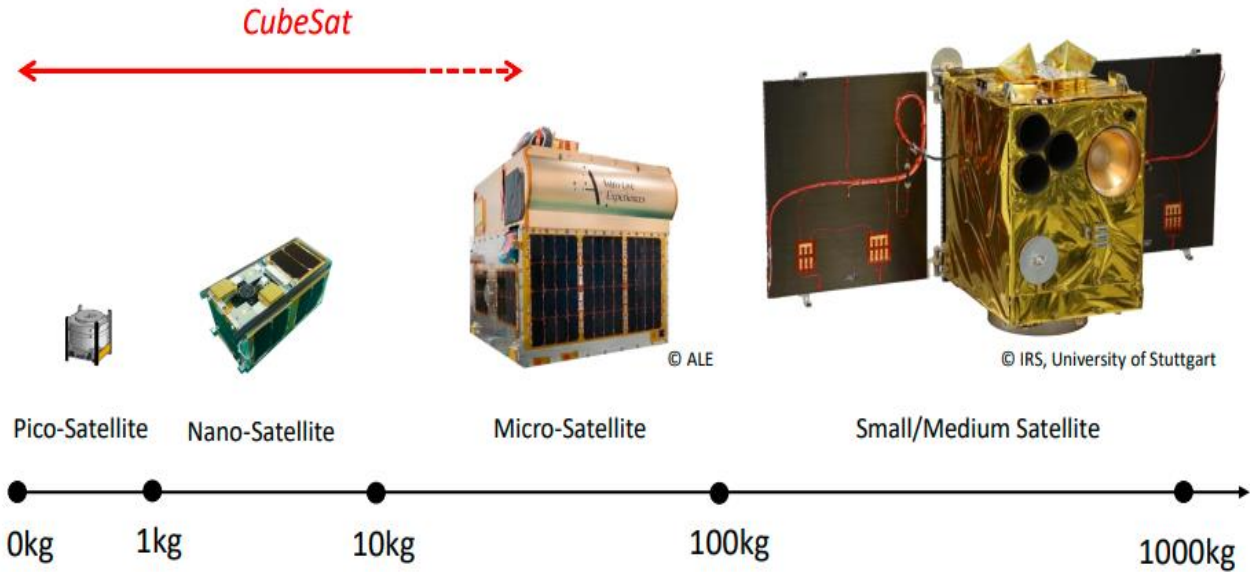


Figure 2 : Mass Categories of Satellites [2].

I.3 Satellite size vs cost and applications

Small satellites, such as CubeSats, have revolutionized the space industry by offering a cost-effective and efficient alternative to traditional large satellites. One of the primary advantages of small satellites is their lower cost, which makes them more accessible to a wider range of organizations and individuals. For example, a CubeSat can be built and launched for as low as \$50,000 to \$150,000, whereas a traditional satellite can cost hundreds of millions of dollars. Additionally, small satellites are more agile and flexible, allowing them to be deployed in constellations and adapted to changing mission requirements. They also offer faster development and deployment times, with some CubeSats being launched within 8 months of development. Furthermore, small satellites are more suitable for Earth observation and remote sensing applications, providing high-resolution imagery and frequent revisits to specific areas on Earth [3].

Here is a table comparing the benefits of small satellites to big ones:

Table 1 : Evaluating the Advantages of Small Satellites Over Big Satellites [3].

Characteristic	Small Satellites	Big Satellites
Cost	\$50,000 - \$150,000	\$100 million - \$300 million
Development Time	8 months	5-15 years
Agility	High	Low
Flexibility	High	Low
Earth Observation	High-resolution imagery, frequent revisits	Low-resolution imagery, infrequent revisits
Launch Complexity	Low	High

I.4 The Evolution of Small Satellite Launches by Weight Class (2010-2022)

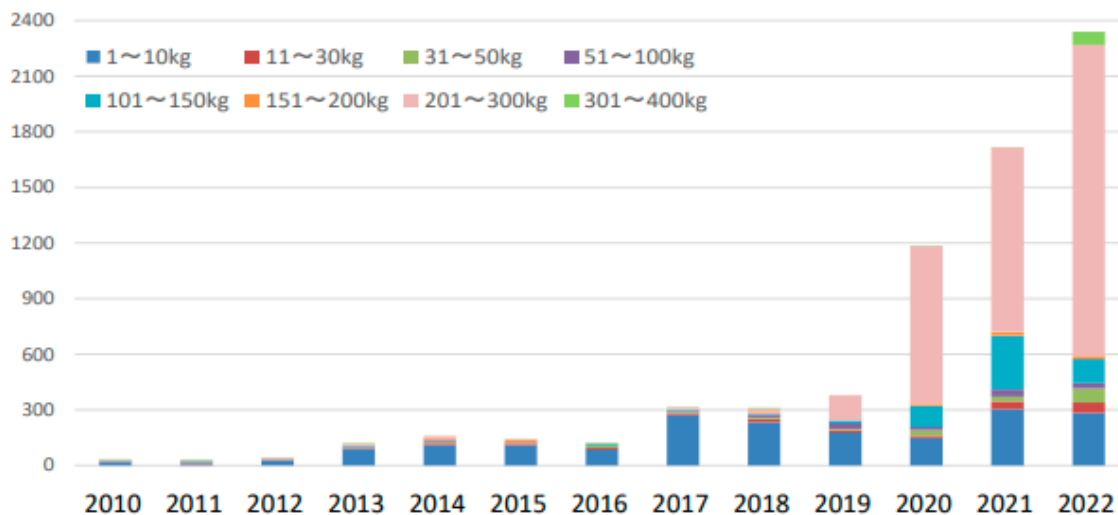


Figure 3 : Launches of Small Satellites (1~400kg) (Successful Launches Only) [2].

The diagram illustrated in Figure 3 showcases a significant acceleration in the utilization of small space systems in the United States over the past decade. The number of launched spacecraft has seen a dramatic rise across various weight categories, with the most notable increase occurring in the 1-10kg range. This surge likely reflects the growing popularity of CubeSats, a type of miniaturized satellite. Several factors might be driving this trend, including advancements that have made small space systems more cost-effective to develop and launch compared to their larger counterparts. Additionally, the faster development cycles associated with these systems allow for quicker innovation and testing in space. Furthermore, the diverse applications of small space systems, ranging from Earth observation and communication to

scientific research, are creating a wider demand for their deployment. This overall trend signifies a growing shift towards a more accessible and dynamic space exploration landscape [2].

I.5 The Rise of CubeSats: Democratization and the Accessibility of Space

The advent of nanosatellite has revolutionized the accessibility of space, making it possible for a wider range of organizations and individuals to participate in space exploration. These small, modular satellites have drastically reduced the costs associated with satellite development and launch, opening up the doors of space to universities, research institutions, and even private companies. This democratization of space exploration has led to a surge in satellite deployments, expanding the reach of Earth-space communication and enabling new constellations and innovative applications [4]. For instance, nanosatellites have been used to monitor climate change, track weather patterns, and provide communication services to remote areas. Additionally, they have enabled the development of new technologies such as satellite-based internet and navigation systems. The reduced costs and increased accessibility of nanosatellites have also made it possible for more countries to participate in space exploration, fostering international cooperation and collaboration [5].

I.6 CubeSat Application

- CubeSats can be used for technology demonstration, testing new instruments or materials and validating their readiness for complex space missions. For example, a CubeSat could be used to study the performance of a new thermal imaging camera by using it with different settings to evaluate the quality of images captured and the overall reliability of the instrument [6].
- CubeSats can also carry small science instruments to conduct experiments or take measurements from space. They can collect information on various phenomena, such as the magnetic field, to better understand and predict its fluctuations in order to improve earthquake detection [6].
- In educational projects, CubeSats can provide students with a unique hands-on experience in developing space missions from design, to launch and operations. For instance, a CubeSat could be used by students to track the movement of wild animals, like herds of reindeer or polar bears, by collecting radio signals emitted from collars attached to the animals [7].

- CubeSats can also be used for commercial applications, such as providing telecommunications services or capturing Earth observation images. A company owning a CubeSat equipped with a camera could sell high-resolution images of the Earth to clients in agriculture, city planning, or business intelligence [7].

I.7 Satellite Subsystems

CubeSats are comprised of several key subsystems, each integral to the satellite's overall functionality and mission success. These subsystems include the Payload System, which carries out the main mission tasks; the Power Control System, which manages power generation and distribution; and the Communication System, which ensures data exchange with ground stations. Additionally, the Command and Data Handling System processes and stores data, while the Structure and Mechanism System provides the physical framework. The Thermal Control System maintains optimal temperatures, the Attitude Control System manages orientation, and the Orbit Control System (advanced) adjusts the satellite's trajectory. Our primary interest lies in the Communication System, as it is crucial for maintaining reliable data transmission and reception, directly impacting the CubeSat's ability to perform its mission effectively [8]. Typical categorization is as follows:

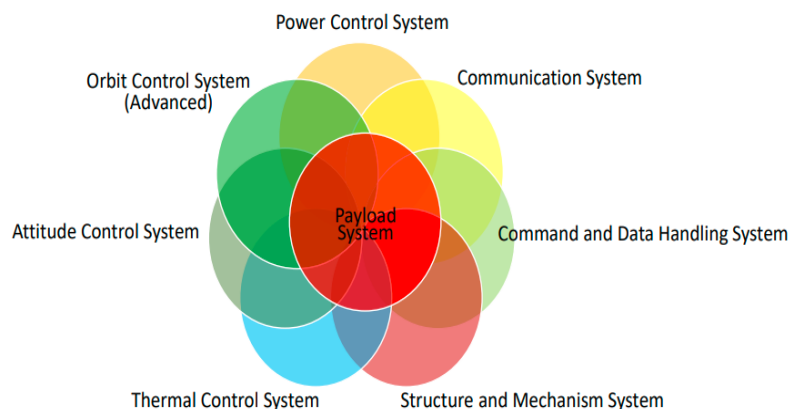


Figure 4 : Satellite Subsystems [8] .

I.8 Communication Sub-system

The communication subsystem is a critical component of a CubeSat, enabling the exchange of information between the satellite and ground stations. It facilitates the transmission of data collected by the CubeSat's payload and the reception of commands from the ground. The subsystem typically consists of a transmitter, antenna, communication channel, and receiver. The transmitter converts data into signals suitable for transmission, while the antenna radiates these signals into space and receives incoming signals. The communication channel,

often the space environment, carries these signals to and from the CubeSat. Finally, the receiver captures the signals and converts them back into usable data. This basic setup ensures that the CubeSat can perform its mission effectively, maintaining continuous and reliable communication with Earth [2].



Figure 5: Basic communication subsystem scheme.

I.8.1 Transmitter/Receivers

As the satellite operates remotely in space, information exchange through communication is indispensable to make the mission of the satellite meaningful. The communication throughput, especially for the down-link, determines and limits the overall performance of the satellite system. For high-speed communication, higher electrical power is required, which increases the temperature of the transmitter. Typically, a ground contact lasts about 10 minutes or less. Ideally, the receiver should be powered on at all times to ensure the satellite does not miss any commands sent from the ground station. The transmitter, however, can be turned on and off according to the ground contact schedule [2].

I.8.2 Antenna

The design and implementation of antennas in CubeSat communication subsystems are critical for ensuring effective data transmission and reception. CubeSats, given their compact size and resource constraints, necessitate the use of antennas that maximize performance while adhering to physical and power limitations [2].

We can classify Cubesat antennas into two classes in term of size and deploibility:

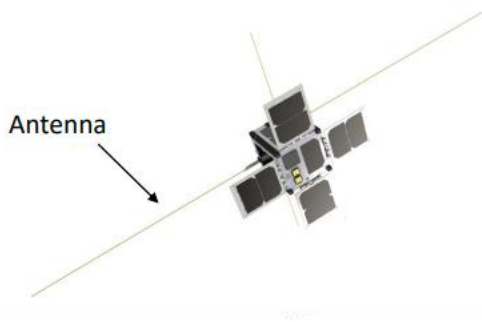


Figure 6 : Low Frequency / Long Wavelength [2].



Figure 7 : High frequency / Short Wavelength [2].



Figure 8:Yagi-Antenna for VHF-band [2].



Figure 9: Dish-Antenna for S-Band [2].

Low frequency antennas, operating within the Very High Frequency (VHF) band, are characterized by their longer wavelengths and lower frequencies. These antennas are essential for CubeSats that require reliable communication over vast distances with moderate data rates. A typical configuration of a low frequency antenna on a CubeSat, as illustrated in Figure 6, involves deploying long, slender rods. These rod-like structures extend from the CubeSat body, enabling the transmission and reception of VHF signals. Such antennas are advantageous due to their relatively simple design and robust performance in VHF communication, which is less susceptible to attenuation and interference compared to higher frequency bands [2].

Supporting the ground segment, the Yagi antenna, as depicted in Figure 8, is a prevalent choice for VHF communications. This antenna type consists of multiple parallel elements aligned in a linear fashion, which helps to focus the signal in a particular direction, thereby enhancing gain and improving communication range. The directional nature of Yagi antennas makes them highly effective for long-range communications, providing a stable link between the CubeSat and the ground station [2].

On the other hand, high frequency antennas operate within the S-band, covering frequencies from 2 to 4 GHz. These antennas are integral for missions that demand high data

rates and enhanced communication capabilities. Due to the shorter wavelengths associated with high frequencies, these antennas can be designed more compactly, which is particularly beneficial for the limited surface area of CubeSats. Figure 7 presents a CubeSat equipped with a high frequency antenna, demonstrating a more compact and sophisticated design [2].

For the ground segment of high frequency communications, dish antennas, exemplified in Figure 9, are widely used. Dish antennas offer significant advantages due to their high directionality, which focuses the signal into a narrow beam, thereby increasing signal strength and reception quality. This characteristic is crucial for S-band communications, where maintaining a strong and clear signal is essential for transmitting large volumes of data efficiently. The ability of dish antennas to concentrate signals makes them ideal for high data rate applications, ensuring robust communication links between the CubeSat and the ground station[2].

I.9 Conclusion

The introduction to nanosatellites and CubeSats has provided a comprehensive overview of the current state of the space industry, highlighting the accessibility of space and the role of small space systems in democratizing access to space. The chapter has discussed the mass categories of satellites, including CubeSats, and their applications in various fields such as Earth observation, communication, and scientific research. The chapter has also explored the cost-effectiveness of CubeSats compared to traditional satellites, making them an attractive option for many organizations and individuals. Additionally, the chapter has touched upon the accelerating utilization of small space systems and the rise of CubeSats as a key player in the space industry. The chapter concludes by highlighting the importance of understanding the various satellite subsystems, including the communication system, which is crucial for effective communication and data transmission. This will be discussed in detail in Chapter 2.

II.1 Introduction

Nanosatellites, particularly CubeSats, have revolutionized space exploration by offering a miniaturized and cost-effective platform for various applications. These spacecraft depend on a set of integrated subsystems to function in space. This chapter, following an overview of these subsystems in the precedent chapter, focuses on the communication subsystem.

This last serves as the lifeline of a CubeSat by enabling data exchange between the spacecraft and ground stations. Effective communication allows for mission control to monitor the health and status of the satellite, receive scientific data collected by onboard instruments, and transmit commands for payload operation and spacecraft manoeuvres. This chapter will comprehensively explore the design considerations, technological advancements, and operational challenges associated with CubeSat communication systems. By analysing various communication architectures, and modulation techniques, we will provide a detailed understanding of the modulation process in our subsystem[9].

The communication system basically deals with the transmission of information from one point to another using the steps, which are carried out in sequential manner. The system for data transmission makes use of the sender and destination address, and this other so many elements that allows to transfer data from one set of point to another set of point, after dividing the elements of communication system in groups. These interface elements acts as the main component for data communication and all these interface elements are given below[9].

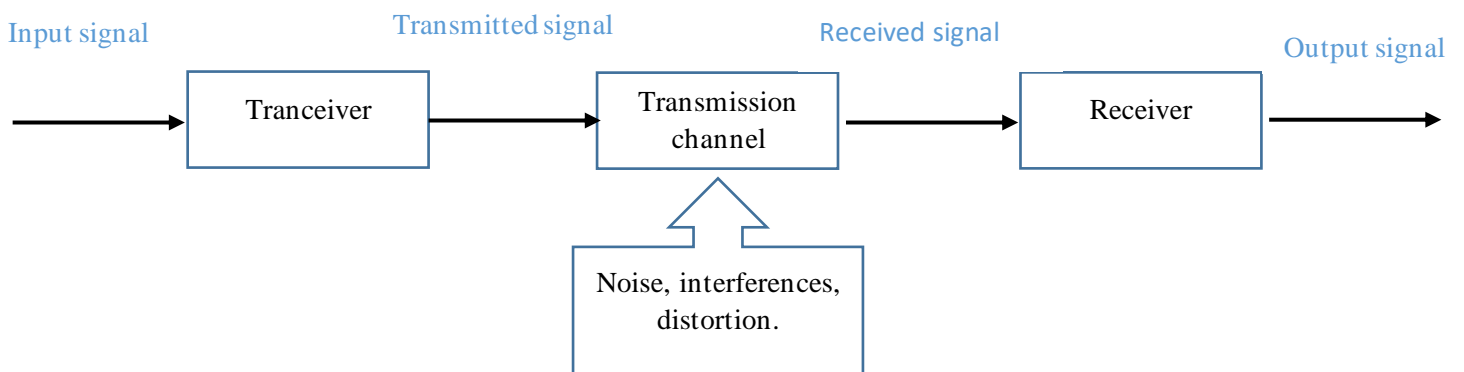


Figure 10 : Communication channel.

The CubeSat communication system is composed primarily of the telemetry and command systems, which send and receive data, respectively. Analog and digital data collected by the sensors and payload of the satellite must be relayed to the ground station via the telemetry system, which is composed of a transmitter that acts much like a “modem in a computer”. The microcontroller will accumulate data from the sensors and convert these inputs into a stream of 8-bit binary numbers. This numerical string is encoded into AX.25² protocol by the ²terminal node controller (TNC)³, which serves to “packetize” the information and key the transmitter. The transmitter then sends the signal to the ground station through the satellite’s antenna. A radio operating in the ultrahigh frequency (UHF) band at the ground station will receive the data signal and encode the stream to a form that may be interpreted by software [9].

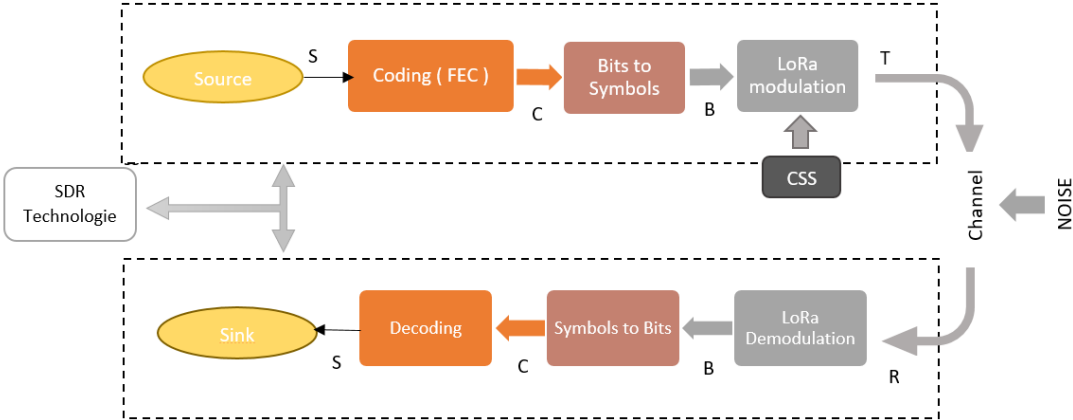


Figure 11: Detailed synoptic diagram for recent communication subsystem.

II.2 Detailed study of the synoptic diagram for the communication Sub-system

II.2.1 Source

The communication process begins with the source, which is the origin of the data to be transmitted. This data, denoted as **S**, could include telemetry data, scientific measurements, or command and control signals generated by the CubeSat's onboard systems. The role of the source is to provide the raw data bits that will be sent through the communication system to a ground station or another satellite.

² AX.25: is a data link layer protocol used in CubeSats for reliable communication over amateur radio frequencies, enabling the transmission of telemetry and commands between the satellite and ground stations.

³ A Terminal Node Controller (TNC): is a device that interfaces between a computer and a radio transceiver, managing data packetization, modulation, demodulation, and error correction for reliable communication.

II.2.2 Coding (FEC)

Once the raw data S is generated, it enters the Forward Error Correction (FEC) block. The purpose of FEC is to add redundancy to the data stream, allowing for the detection and correction of errors that may occur during transmission. This process involves encoding the source data S into channel-coded bits C using an encoding function:

$$C = \text{Encode}(S) \quad (1)$$

Forward Error Correction (FEC) is a method used in communication systems to detect and correct errors in transmitted data. By adding redundant data to the original message, FEC enables the receiver to identify and correct errors without needing a retransmission, ensuring more reliable communication even over noisy or unstable channels [10].

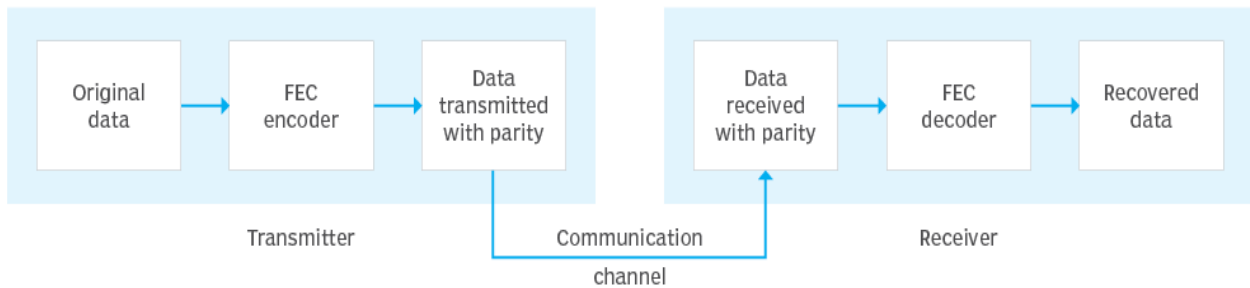


Figure 12: FEC (Forward Error Correction) channel [10].

II.2.2.1 Example of the process in Forward Error Correction protocol

The FEC protocol Principle is to add extra bits to transmitted data to catch and fix errors. The "1/2" and "1/3" labels show how much extra data is added compared to the original. For example, in 1/2 FEC, one extra bit is added for every two bits of original data, while in 1/3 FEC, two extra bits are added for every three original bits. This helps receivers correct mistakes without needing to ask for the data again. Higher FEC rates offer better error fixing but use more space. So, the choice depends on balancing error fixing and space use [10].

II.2.3 Bits to Symbols (Mapping)

The channel-coded bits C are then mapped to modulation symbols in the Bits to Symbols block. Each group of bits is converted into a corresponding symbol according to the modulation scheme used by LoRa. This process can be represented by the mapping function:

$$\mathbf{B} = \text{Map}(\mathbf{C}) \quad (2)$$

This transformation prepares the data for the modulation stage, converting it into a format suitable for transmission.

II.2.4 LoRa Modulation

The next step is LoRa modulation using Chirp Spread Spectrum (CSS) technology. The mapped symbols \mathbf{B} are modulated into a transmitted signal \mathbf{T} .

CSS spreads the signal over a wide frequency range, which makes it robust against interference and capable of long-range transmission. This step is crucial for ensuring that the signal can travel the long distances required in space communication [11].

II.2.4.1 Why Lora modulation?

LoRa modulation is chosen for its ability to provide long-range communication with low power consumption, LoRa's robustness against interference and its ability to operate in unlicensed frequency bands make it highly reliable and cost-effective for satellite communication projects. In this section we gonna have a depth study of the LoRa modulation.

II.2.4.2 Overview of the CSS modulation

Chirp Spread Spectrum (CSS) modulation is a key component of LoRa technology. It converts the data to be transmitted into a series of chirps signals that vary in frequency over time. CSS provides robustness against interference and multipath fading, making it suitable for long-range, low-power communication [11].

II.2.4.3 LoRa Spread Spectrum

In LoRa modulation, spectrum spreading is achieved by generating a chirp signal that continuously varies in frequency. This method offers the advantage of equating timing and frequency offsets between the transmitter and receiver, significantly reducing the complexity of the receiver design. The frequency bandwidth of the chirp matches the spectral bandwidth of the signal, ensuring efficient and reliable communication [11].

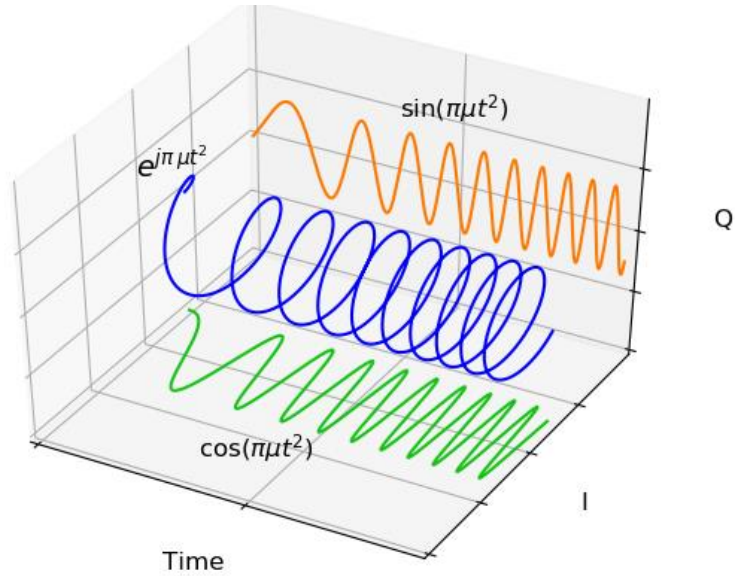


Figure 13: Chirp Propagation Wave [12].

The figure illustrates the components of a chirp signal in LoRa modulation, showing the time evolution of its in-phase (I) and quadrature (Q) components. The green curve represents $\cos(\pi\mu t^2)$, the orange curve represents $\sin(\pi\mu t^2)$, and the blue curve represents the complex exponential $e^{j\pi\mu t^2}$, combining the real and imaginary parts. This chirp signal, with its linearly increasing frequency, is fundamental to LoRa's chirp spread spectrum technology [11].

Where μ : chirp rate.

II.2.4.4 Mathematical Equation for The SIGNAL $T(n)$

Based on the above process, the equation for signal $T(n)$ can be written as:

$$T(n) = \frac{1}{\sqrt{2^{SF}}} e^{j.2\pi\left(\frac{n^2}{2^{SF+1}}\right)} \quad (3)$$

where:

- SF is the spreading factor (7..12).
- n ranges from 0 to $\{2^{SF} - 1\}$.

It is important to note that this equation is provided by the developer of this modulation (i.e. Lora) [11].

- **Spreading Factor** The spreading factor dictates the rate at which a chirp progresses. The duration of a chirp is approximately equal to 2^{SF} . As illustrated in the spectrogram below, each increment in the spreading factor nearly doubles the chirp's duration and its range [11].

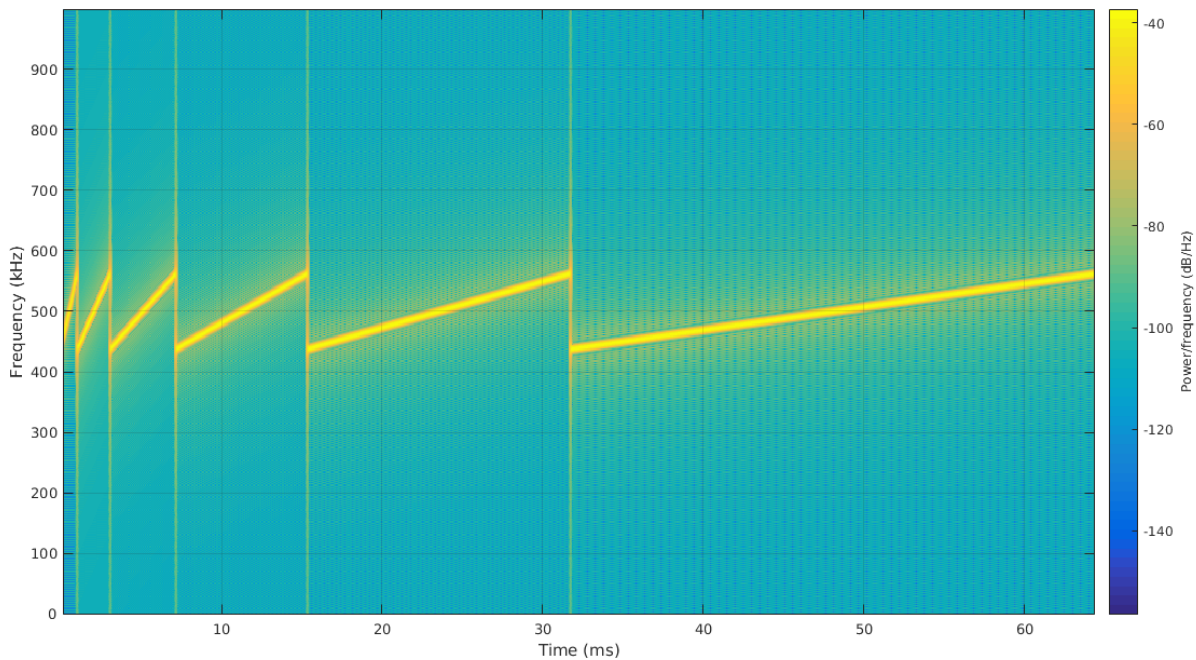


Figure 14 : Comparison Of the Lora Spreading Factors SF=7 to SF=12 [13].

In this chart Figure 14, we demonstrate how varying the spreading factor within the same frequency band can impact propagation performance.

II.2.4.5 Impact of Spreading Factor (SF) on LoRa Communication

The Spreading Factor (SF) in LoRa modulation plays a crucial role in determining the communication range, data rate, and noise resilience of the system. Essentially, the SF defines how many chirps are used to encode each bit of information. A higher SF, such as SF12, involves a greater number of chirps per bit, which results in improved signal processing gain. This enhancement enables the system to maintain reliable communication over longer distances. Furthermore, higher SFs help in distinguishing the signal from background noise more effectively, thereby increasing the robustness of the communication link in noisy environments. However, it's important to note that as the SF increases, the data rate decreases, leading to a trade-off between range and data throughput[30][31].

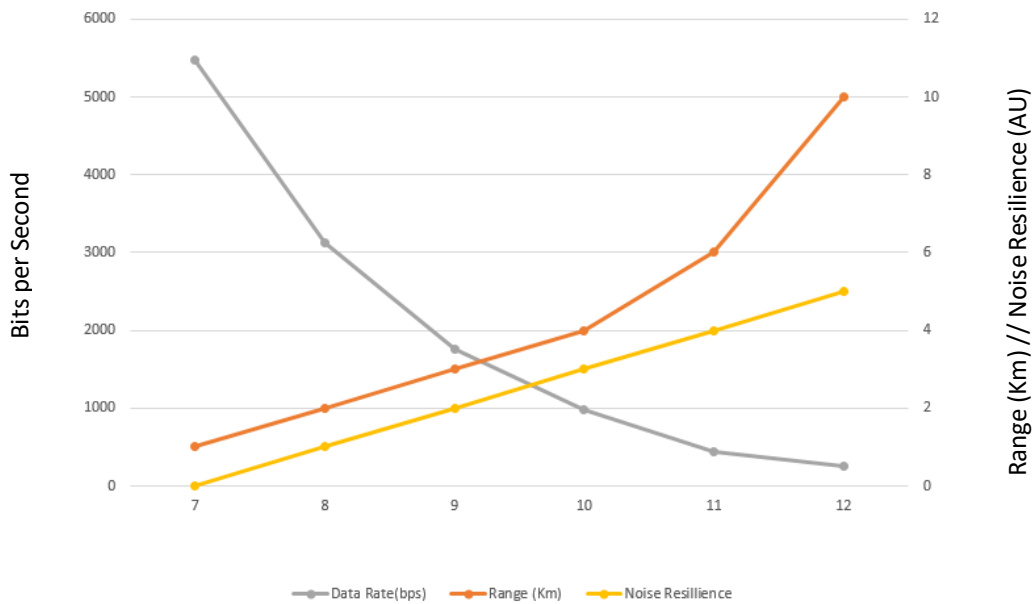


Figure 15 : graph illustrates the impact of the Spreading Factor (SF) on range, data rate, and noise resilience in LoRa communication [30][31].

II.2.4.5.1 Range

Range, measured in kilometers (Km), refers to the distance over which data can be effectively transmitted. In the graph, the range shows a consistent and significant increase as the value rises from 7 to 12. Starting at value 7, the range is just over 1 Km, indicating a limited transmission distance. However, as the value increases, the range expands steadily. By value 8, the range reaches around 2 Km, continuing to increase linearly to approximately 6 Km by value 11. The most dramatic increase occurs between values 11 and 12, where the range jumps sharply to 10 Km. This trend suggests that higher values greatly enhance the system's ability to transmit data over longer distances. Such a feature is crucial for applications where long-distance communication is essential. However, the extended range comes at the cost of reduced data rate and potentially other performance metrics, necessitating a careful balance based on specific use-case requirements, see *Figure 15* [30][31].

II.2.4.5.2 The data rate

The data rate, measured in bits per second (bps), indicates how quickly data can be transmitted over a communication system. In the graph, the data rate shows a clear downward trend as the value increases from 7 to 12. At value 7, the data rate is at its highest, approximately

5000 bps, suggesting a robust capacity for rapid data transmission. However, as the value progresses, the data rate declines sharply. By value 8, it drops to around 4000 bps, and continues to decrease linearly to about 1000 bps at value 10. Beyond value 10, the rate of decline slows, reaching slightly below 500 bps by value 12. This significant reduction in data rate as the value increases suggests that certain factors, likely linked to the range and noise resilience, impose limitations on the speed of data transmission. In practical terms, this means that for applications requiring high-speed data transfer, lower values are more suitable, but this comes with trade-offs in other areas such as range and noise resilience, see Figure 15 [30][31].

II.2.4.5.3 Noise resilience

Noise resilience, often measured in terms of decibels (dB) or other units, indicates a system's capability to maintain data integrity in the presence of noise. The graph shows that noise resilience improves steadily as the value increases from 7 to 12. At value 7, noise resilience is minimal, close to 0, suggesting poor performance in noisy environments. As the value increases, noise resilience grows linearly, reaching about 2.5 at value 10 and approximately 4 by value 12. This trend highlights that higher values correspond to better noise handling capabilities, allowing the system to function more reliably in environments with significant interference. Enhanced noise resilience is vital for maintaining data accuracy and reducing errors, particularly in real-world scenarios where noise is a common issue. Therefore, systems designed for high-noise environments would benefit from higher values, though this comes with a reduction in data rate, see Figure 15 [30][31].

II.2.4.6 Up-Chirp and Down-Chirp Signals

In LoRa modulation, data encoding utilizes both up-chirps and down-chirps, which differ primarily in the direction of their frequency sweep over time. An up-chirp increases in frequency as time progresses, while a down-chirp decreases in frequency over the same period. The mathematical representation of these signals reflects this fundamental difference. An up-chirp can be described by a signal whose instantaneous frequency linearly increases with time, whereas a down-chirp's instantaneous frequency linearly decreases. This distinction in frequency behavior is crucial for encoding and decoding data, as the direction of the chirp sweep affects how the information is processed and interpreted by the receiver. Understanding the nuances between up-chirps and down-chirps is essential for optimizing LoRa communication systems, as it impacts the overall efficiency and reliability of data transmission [14].

II.2.4.6.1 Characteristics of Up-Chirp

- An up-chirp signal increases its frequency linearly over time.
- The quadratic phase term $\frac{n^2}{2SF+1}$ is positive, indicating that the frequency increases as n increases.

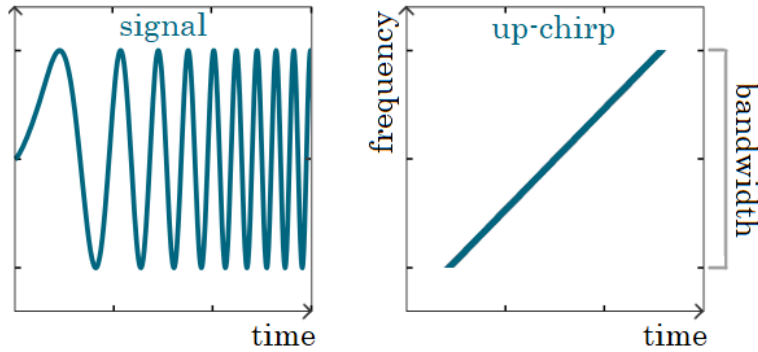


Figure 16 : UP chirp Signal [14].

II.2.4.6.2 Comparison with Down-Chirp

- For a down-chirp, the quadratic term would have a negative coefficient, indicating that the frequency decreases over time.
- The mathematical representation for a down-chirp would typically have the form:

$$T(n) = \frac{1}{\sqrt{2SF}} e^{-j.2\pi\left(\frac{n^2}{2SF+1}\right)} \quad (4)$$

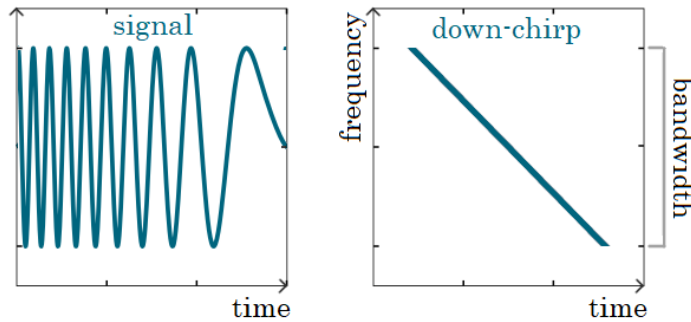


Figure 17 : DOWN chirp Signal [14].

II.2.4.7 Lora modulation coding

LoRa modulation, data encoding is achieved through cyclically shifted chirps, where the frequency jumps determine the encoded information. Let's explore how the spreading factor (SF) is utilized in LoRa to encode messages [15].

Consider a symbol consisting of the binary sequence 1011111, which represents the decimal value 95.

- The number of raw bits to be encoded by one symbol is 7.
- Therefore, the Spreading Factor (SF) is 7.

With $SF = 7$, the symbol has 2^{SF} possible values, this gives us a range from 0 to 127.

The symbol value is encoded onto a sweep signal (up-chirp). This sweep signal is divided into $2^{SF} = 128$ chips. This process is illustrated in the Figure 17 below [15]:

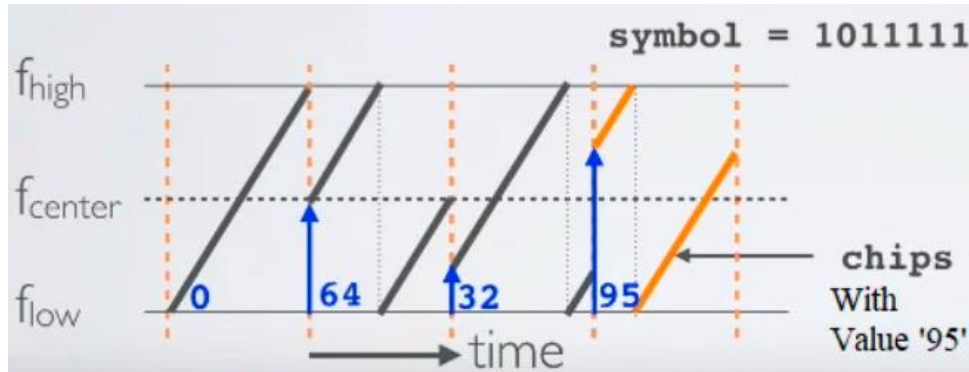


Figure 18 : Chirp Spread Spectrum Coding Process [15].

The wanted data signal is chipped at a higher data rate and modulated onto the chirp signal.

II.2.4.8 LoRa modulation characteristics

The relationships between data bit rate, symbol rate, and chip rate in LoRa modulation are defined by specific equations involving the spreading factor (SF) and bandwidth (BW):

- **Modulation Bit Rate (Rb):**

The rate at which data bits are transmitted is given by:

$$Rb = SF * \frac{1}{\left[\frac{2^{SF}}{BW}\right]} \text{ bits/sec} \quad (5)$$

Where:

- SF = spreading factor (7..12)
- BW = modulation bandwidth (Hz)

This equation shows that the bit rate Rb is directly proportional to the spreading factor and the bandwidth [11].

- **Symbol Period (Ts):**

The time taken to transmit one symbol is:

$$Ts = \frac{2^{SF}}{BW} \text{ secs} \quad (6)$$

~ 29 ~

- **Symbol Rate (Rs):**

The symbol rate, the reciprocal of the symbol period, is:

$$R_s = \frac{1}{T_s} = \frac{BW}{2^{SF}} \text{ symbols/sec} \quad (7)$$

This relationship shows that the symbol rate is inversely proportional to the spreading factor and directly proportional to the bandwidth [11].

- **Chip Rate (Rc):**

The rate at which chips are transmitted is: In LoRa modulation, the chip rate Rc is defined as the rate at which chips (basic modulation units) are transmitted. Since LoRa modulation uses one chip per second per Hz of bandwidth, the chip rate can be derived from the symbol rate [11]:

$$R_c = R_s * 2^{SF} \quad (8)$$

$$R_c = \frac{BW}{2^{SF}} * 2^{SF} \text{ chips/sec} \quad (9)$$

- **Nominal Bit Rate (Rb):**

The nominal bit rate of the data signal, accounting for error correction, is: LoRa modulation includes a variable error correction scheme to improve the robustness of the transmitted signal. This introduces redundancy, which affects the nominal bit rate. The nominal bit rate Rb of the data signal can be defined as [11]:

$$R_b = SF * \frac{\left[\frac{4}{4+CR} \right]}{\left[\frac{2^{SF}}{BW} \right]} \quad (10)$$

Where:

- SF = spreading factor (7..12)
- CR = code rate (1..4)
- BW = modulation bandwidth (Hz)

Here, CR is the code rate (ranging from 1 to 4). This equation shows that higher spreading factors or stronger error correction (higher CR) result in lower bit rates due to increased redundancy [11].

II.2.4.9 LoRa physical layer

In case of reaching a reliable data transmission in long-distance, it's important to study the LoRa frame, and in how its composed.

The LoRa PHY (Physical Layer) frame is composed of several fields that facilitate the transmission of data between devices. The primary components of a LoRa PHY frame include the preamble, header, payload (data), and CRC (Cyclic Redundancy Check)[16]. As in *Figure 19*.



Figure 19 : LoRa physical Frame.

The frame begins with a **preamble**, which is a sequence of identical symbols used to help the receiver recognize the start of a new packet and synchronize with the transmitter's timing. The length of the preamble can be configured based on the requirements of the communication protocol.

Following the preamble is **the header**, which provides essential information about the frame's structure, such as the payload length, forward error correction (FEC) rate, and the presence of an optional CRC. There are two types of headers: explicit and implicit. The explicit header, included in the frame, contains metadata and is particularly useful for applications with frequently changing packet structures. The implicit header is used when the transmitter and receiver have pre-agreed on the frame's structure, reducing overhead.

The **payload** is the actual data being transmitted. Its length can vary depending on the application and the configuration of the LoRa parameters. To enhance the robustness of the transmission, LoRa employs Forward Error Correction (FEC), which adds redundancy to the data, improving its resistance to errors.

Finally, the **Cyclic Redundancy Check (CRC)** is an optional field that provides error detection for the payload. If enabled, the CRC allows the receiver to verify the integrity of the received data, ensuring that it has not been corrupted during transmission. The CRC is calculated over the payload and, if present, the header, and its length is 2 bytes.

II.2.4.10 LoRa Link Budget

In the context of LoRa modulation used in the CubeSat communication subsystem, the link budget measures all the gains and losses from the transmitter, through the propagation channel, to the target receiver. This includes system gains and losses associated with antennas, matching networks, and losses related to the propagation channel itself, whether modeled or based on measured data. Randomly varying channel mechanisms, such as multipath and Doppler fading, are addressed by adding a margin that reflects the expected severity of these effects [11].

The link budget for a CubeSat's communication link can be expressed as:

$$P_{RX}(dBm) = P_{TX}(dBm) + G_{system}(dB) - L_{SYSTEM}(dB) - L_{CHANNEL}(dB) - M(dB) \quad (12)$$

Where:

- P_{RX} = the expected power incident at the receiver.
- P_{TX} = the transmitted power.
- G_{SYSTEM} = system gains such as those associated with directional antennas, etc.
- L_{SYSTEM} = losses associated with the system such as feed-lines, antennas (in the case of electrical short antennas associated with many remote devices), etc.
- $L_{CHANNEL}$ = losses due to the propagation channel, either calculated via a wide range of channel models or from empirical data.
- M = fading margin, again either calculated or from empirical data.

A communication channel is said to be link limited when the losses associated with the channel cause the incident power level at the receiver to fall below that required to meet the SNR requirement of the receiver for correct demodulation of the received data. This scenario can critically impact the performance and reliability of the CubeSat communication subsystem [11].

II.2.4.11 Comparative Analysis of FSK and LoRa

Frequency Shift Keying (FSK) and LoRa (Long Range) are two modulation schemes often considered for CubeSat communications due to their distinct characteristics and capabilities. FSK, a traditional modulation method, is valued for its simplicity and robustness. In contrast, LoRa, a relatively newer technology, offers exceptional long-range communication capabilities, making it suitable for various low-power, long-range applications. This analysis explores the comparative advantages of FSK and LoRa in the context of CubeSat communication subsystems, focusing on range, sensitivity, and data rate [17].

Table 2 : Link Budget comparison LoRa vs FSK [17].

Mode	Bit rate (kb/s)	Sensitivity (dBm)	Δ (dB)
FSK	1.2	-122	-
LoRa SF=12	0.293	-137	+15
LoRa SF=12	0.537	-134.5	+12.5
LoRa SF=12	0.976	-132	+10
LoRa SF=12	1.757	-129	+7
LoRa SF=12	3.125	-126	+4
LoRa SF=12	5.468	-123	+1
LoRa SF=12	9.375	-118	-3

II.2.4.11.1 Range

LoRa technology is well-known for its long-range capabilities, often achieving communication distances up to 15 kilometers (9.3 miles) in rural areas and between 2 to 5 kilometers (1.2 to 3.1 miles) in urban environments. This impressive range is primarily attributed to its Chirp Spread Spectrum (CSS) modulation, which spreads the signal over a wider bandwidth, enhancing its robustness against noise and interference. The spread spectrum technique also aids in better propagation through buildings and obstacles, making LoRa suitable for various long-range applications [17], see *Table 2*.

II.2.4.11.2 Sensitivity

LoRa receivers are extremely sensitive, with sensitivity levels reaching as low as -137 dBm. This high sensitivity is one of the critical factors enabling LoRa's long-range communication capabilities. The CSS modulation used in LoRa allows the receiver to detect very weak signals, and the spreading factor (SF) can be adjusted to trade-off between sensitivity and data rate. This high sensitivity allows LoRa to operate effectively in environments with low signal strength, making it ideal for applications requiring reliable communication over long distances or in challenging conditions [17], see *Table 2*.

FSK receivers, on the other hand, typically exhibit lower sensitivity compared to LoRa, with sensitivity levels around -120 dBm to -125 dBm. FSK modulation does not benefit from the spreading gain that CSS provides, limiting its sensitivity. As a result, FSK is less effective in low-SNR environments and has reduced range and reliability in challenging conditions when compared to LoRa [17].

II.2.4.11.3 Data Rate

LoRa offers variable data rates ranging from 0.3 kbps to 50 kbps. The data rate is inversely proportional to the spreading factor (SF); higher SF values provide better sensitivity and range but result in lower data rates. This flexibility allows for optimizing the data rate based on the application's requirements. Lower SF values increase the data rate but decrease the range and sensitivity. LoRa is particularly suitable for low-data-rate applications such as environmental monitoring, smart agriculture, and IoT devices where long-range and low power consumption are prioritized over high data throughput [17], see *Table 2*.

II.2.4.12 Power Consumption and Sleep Mode in LoRa Modules for CubeSat Systems

II.2.4.12.1 Overview of Power Consumption

LoRa (Long Range) modules are widely recognized for their efficient power consumption, making them an ideal choice for CubeSat communication systems where energy resources are limited. The power consumption of LoRa modules varies significantly based on their operating mode, which includes transmission, reception, and sleep modes.

- **Transmission Power Consumption:** [18].
 - LoRa modules can transmit at different power levels, often ranging from low milliwatts (mW) to higher power levels up to 20 dBm or more, depending on the specific module.
 - The power consumption during transmission depends on the configured output power. For example, a typical LoRa module transmitting at maximum power (e.g., 20 dBm) might consume between 100 to 150 mA.
 - Lower transmission power settings significantly reduce current draw, helping to conserve battery life.

- **Reception Power Consumption:** [18].
 - In receive mode, LoRa modules consume considerably less power compared to transmission mode. Typical current consumption in receive mode ranges from 10 to 15 mA.

- The reduced power consumption during reception is beneficial for systems that spend more time listening for incoming signals than transmitting data
- **Sleep Mode Power Consumption:** [18].
 - LoRa modules support low-power sleep modes that are crucial for energy conservation, especially in space missions where power is a scarce resource.
 - In sleep mode, the module's power consumption can drop to microampere (μA) levels, often as low as 1 to 10 μA , dramatically reducing overall power usage during periods of inactivity.
 - This low-power state is achieved by shutting down most of the internal circuits, leaving only essential components active.

Sleep Mode in LoRa Modulation

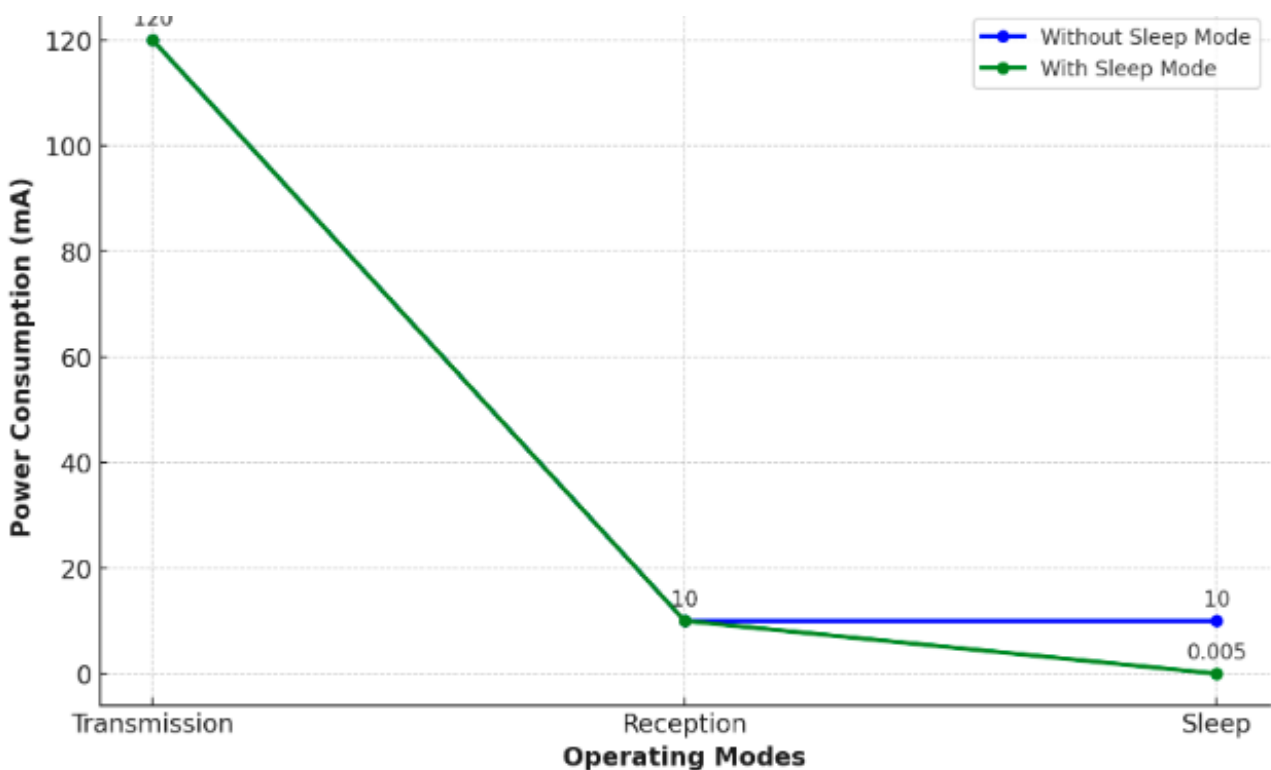


Figure 20 : power consumption comparison without sleep mode vs with sleep mode.

Sleep mode is a crucial power-saving feature in LoRa (Long Range) communication systems, particularly valuable in applications with limited energy resources, such as CubeSat systems.

By utilizing sleep mode, devices can significantly reduce their power consumption when not actively transmitting or receiving data, thereby extending the operational lifespan of battery-powered systems [18].

II.2.4.12.2 How Sleep Mode Works in LoRa Modulation

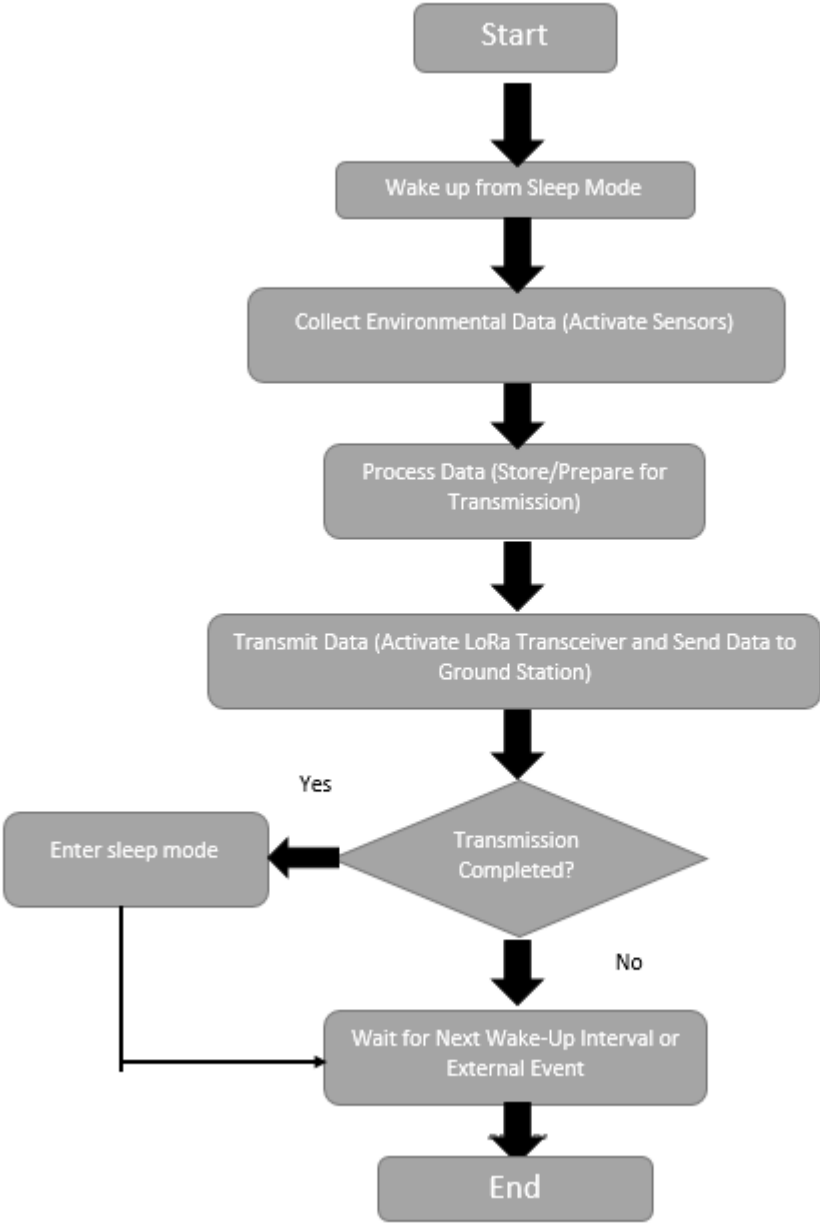


Figure 21: Sleep Mode Principe.

This flowchart illustrates a power-efficient operational cycle for a LoRa-based CubeSat communication system. By effectively utilizing sleep mode during periods of inactivity, the system can significantly reduce its power consumption, extending the operational lifespan of the CubeSat’s battery and ensuring reliable performance throughout the mission. The cycle of

waking up, collecting data, transmitting it, and returning to sleep mode highlights the balance between active communication and energy conservation[18].

Unlike traditional hardware-based radios, SDRs utilize software to perform signal processing tasks, allowing for real-time updates and modifications to communication protocols and frequencies. This capability is particularly advantageous for CubeSats, which are constrained by size, weight, and power limitations. By leveraging SDR technology, CubeSats can dynamically adjust to varying communication requirements and environmental conditions in space, enhance signal clarity and strength, and support multiple communication standards with a single hardware setup. The implementation of SDR in CubeSat communication subsystems not only optimizes the performance and reliability of these small satellites but also significantly reduces development costs and time, paving the way for more innovative and cost-effective space missions [19].

II.2.5 Introduction to Software Defined Radio (SDR) and its Integration in CubeSat Communication Systems

This section provides an overview of SDR technology, Software Defined Radio technology has emerged as a pivotal innovation in modern communication systems, offering versatile capabilities and enhanced flexibility compared to traditional hardware-centric approaches. SDR enables the implementation of communication protocols and signal processing tasks through software, allowing for dynamic adaptation to diverse operational requirements. This integration of software-based functionalities within radio systems has revolutionized the field, particularly in the context of CubeSat communication systems [19].

CubeSat communication systems demand efficient and adaptable solutions to facilitate reliable data transmission. SDR presents a compelling option for addressing these challenges, offering inherent advantages such as reconfigurability, scalability, and compatibility with evolving communication standards [19].

Here are examples of successful SDR integration in CubeSat missions:

- **Radiation Monitoring CubeSat (RadSat):** The RadSat mission utilized SDR technology to implement a flexible and adaptive communication system for monitoring radiation levels in Earth's atmosphere. By leveraging SDR's reconfigurability, RadSat could adjust its communication protocols and

frequency bands based on real-time radiation data, ensuring reliable transmission and reception despite changing environmental conditions [19].

- **CubeSat for Ionospheric Scattering Observations (CISO):** CISO⁴ employed SDR platforms to enable multi-mode communication capabilities for studying ionospheric scattering phenomena. The SDR-based transceiver onboard CISO facilitated the implementation of various modulation schemes and signal processing techniques, allowing for comprehensive analysis of ionospheric disturbances and their impact on radio wave propagation [20].

These SDR devices have been successfully deployed in CubeSat missions, demonstrating their effectiveness in enabling flexible and adaptable communication systems for small satellite platforms.

Here are some examples of SDR devices that have been used in CubeSat projects.

II.2.5.1 LimeSDR Mini

- The LimeSDR Mini is a compact and low-cost SDR platform that has been used in CubeSat experiments and educational projects [21].



Figure 22 : LimeSDR Mini [21].

II.2.5.2 HackRF One

- The HackRF One is a popular open-source SDR platform developed by Great Scott Gadgets. Its frequency range (1 MHz to 6 GHz) and wide bandwidth (up to 20 MHz) make it suitable for a variety of CubeSat communication and sensing applications [22].

⁴ CISO: CubeSat for Ionospheric Scattering Observations (CISO) is a small satellite designed to study and monitor the scattering of radio waves in the Earth's ionosphere.



Figure 23 : HackRF One[22].

II.2.6 Channel

The channel represents the medium through which the signal is transmitted from the CubeSat to the ground station. This medium could be a vacuum, atmosphere, or space, and it introduces various impairments to the signal, such as noise, attenuation, and interference. The channel is the primary source of errors in the communication system.

In the context of LoRa modulation for a CubeSat communication system, the primary considerations are typically thermal noise.

II.2.7 LoRa Demodulation

The input to the LoRa demodulation block is the received modulated signal (denoted as R), which has been affected by noise and possibly other distortions during transmission. This signal is typically in the form of chirp signals that have varying frequencies. And it can be expressed as follows:

$$R(n) = T(n) + N(n) \quad (11)$$

Where the $N(n)$ express the noise added in the channel.

The demodulator correlates the received signal with reference chirp signals to extract the transmitted symbols. This involves a process of de-chirping, which effectively reverses the frequency modulation applied during transmission.

The output of the demodulation block is a sequence of symbols. Each symbol represents a unique value that corresponds to a specific bit pattern.

II.2.8 Symbols to Bits:

The input to this block is the sequence of symbols obtained from the demodulation block. This block converts the demodulated symbols back into bits. Each symbol represents a

specific sequence of bits, depending on the spreading factor used in LoRa modulation. This block decodes the symbols by mapping them back to their corresponding bit sequences.

The output is a stream of bits that represent the original coded data before modulation.

$$\{b_1, b_2, b_3 \dots b_m\}$$

Where b_i are the individual bits.

II.2.9 Decoding

The decoding block receives the bit stream output from the symbol to bit conversion process. Decoding involves applying error correction algorithms (such as Forward Error Correction - FEC) to correct any errors introduced during transmission. This step ensures data integrity by detecting and correcting errors in the bit stream.

The result is a stream of bits that closely approximates the original data generated by the source, with errors corrected.

II.2.10 Sink

The sink is the final block in the communication system, representing the destination of the transmitted data. In the context of a CubeSat, the sink is typically the ground station or any onboard system that utilizes the transmitted data for further processing or analysis.

II.3 Conclusion

In this chapter, we have comprehensively examined the CubeSat communication system, starting with an introduction that underscores the importance of efficient and reliable communication for mission success. We discussed the versatility of Software-Defined Radio (SDR) in CubeSat systems, highlighting its ability to adapt to various protocols and frequencies through software updates, and emphasized the role of Forward Error Correction (FEC) in ensuring data integrity by allowing error detection and correction without retransmission. Our detailed analysis of LoRa modulation revealed its suitability for CubeSat communications due to its long-range capabilities and low power consumption.

III.1 Introduction

This chapter explores the implementation of LoRa (Long Range) communication in CubeSats by first simulating the modulation concept using MATLAB to analyse key performance aspects like sensitivity, data rate, and range. Following this, the design is translated into a practical printed circuit board (PCB) using EasyEDA, an online design tool. This process involves creating the circuit schematic, laying out the PCB, and selecting appropriate components such as microcontrollers, transceivers, antenna and sensors.

III.2 LoRa performance with deferent Spreading Factors

The performance of LoRa modulation is influenced by the Signal-to-Noise Ratio (SNR) and the Spreading Factor (SF). SNR affects the noise level in the communication channel, while SF determines chirp symbol duration and data rate. This study simulates LoRa performance under varying SNR values and SFs using MATLAB, analyzing their impact on the symbol error rate (SER) to understand the robustness and reliability of LoRa communication. The MATLAB code and results are discussed in the following sections.

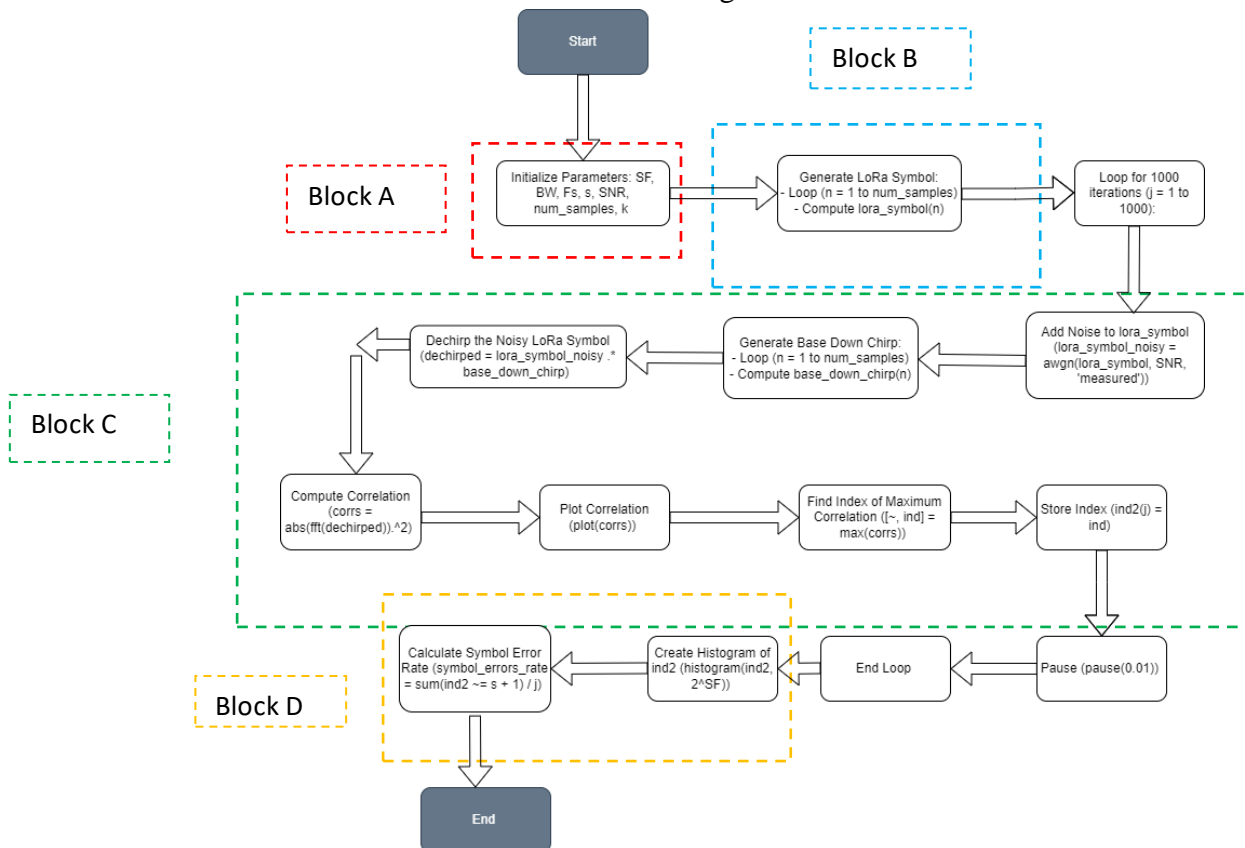


Figure 24 : Matlab Code Organigramme.

Block A: Initialization

The first part of the code initializes several key parameters. The SF is set to 7, which determines the spreading factor used in the LoRa modulation. The BW and Fs are both set to 1000 Hz, representing the bandwidth and sampling frequency, respectively. The variable *s* is defined as 33, representing the symbol to be transmitted, and the SNR is set to -13 dB, specifying the signal-to-noise ratio for the simulation. The number of samples per symbol, *num_samples*, is calculated using the formula $2^{SF} * Fs / BW$, which depends on the spreading factor, sampling frequency, and bandwidth.

Block B: Generate LoRa Symbol

In this part of the code, the LoRa symbol corresponding to the symbol *s* is generated. The variable *k* is initialized to the value of *s*, and the *lora_symbol* array is preallocated with zeros. The code then enters a loop that runs for *num_samples* iterations. Within each iteration, *k* is incremented and reset if it exceeds 2^{SF} , ensuring it stays within the valid range. The LoRa symbol is generated using the formula which creates a complex chirp signal based on the current value of *k*.

$$T(n) = \frac{1}{\sqrt{2^{SF}}} e^{j \cdot 2\pi \left(\frac{n^2}{2^{SF+1}} \right)} \quad (12)$$

Block C: Add Noise and Demodulate

The next section of the code simulates the transmission and reception of the LoRa symbol with added noise. A loop runs for 1000 iterations to gather statistical data. Within each iteration, the *awgn* function is used to add white Gaussian noise to the LoRa symbol, based on the specified SNR.

A base down-chirp signal is then generated in a manner similar to the LoRa symbol, but with an inverse frequency sweep. The received noisy LoRa symbol is multiplied by the base down-chirp to dechirp the signal.

The Fast Fourier Transform (FFT) of the dechirped signal is computed, and its magnitude squared is taken to obtain the correlation values. The index of the maximum correlation value indicates the detected symbol, which is stored in the array *ind2*. The *pause* (0.01) function is included to allow the plot to update in real-time during each iteration.

Block D: Plot Histogram and Calculate SER

After completing the 1000 iterations, a histogram of the detected symbols is plotted using `histogram(ind2, 2^SF)`. This histogram provides a visual representation of the detection accuracy.

Finally, the Symbol Error Rate (SER) is calculated by comparing the detected symbols to the transmitted symbols. The expression $\text{sum}(\text{ind2} \sim s + 1) / j$ computes the proportion of incorrectly detected symbols, accounting for MATLAB's 1-based indexing.

III.3 Simulation Results

- SF = 7 (Low SF)

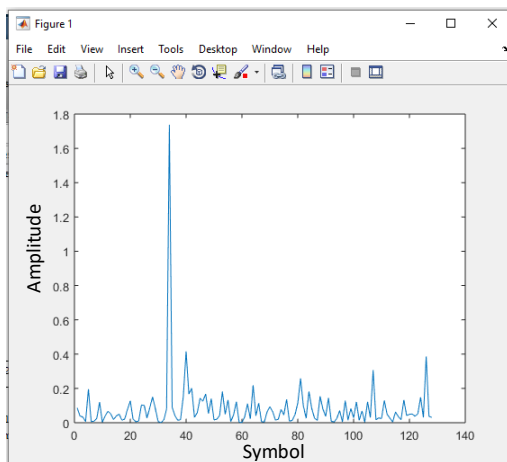


Figure 25 : SER for SF =7 and SNR = -10.

```
Command Window

SNR =

    -10

symbol_errors_rate =

    0.0390

fx >>
```

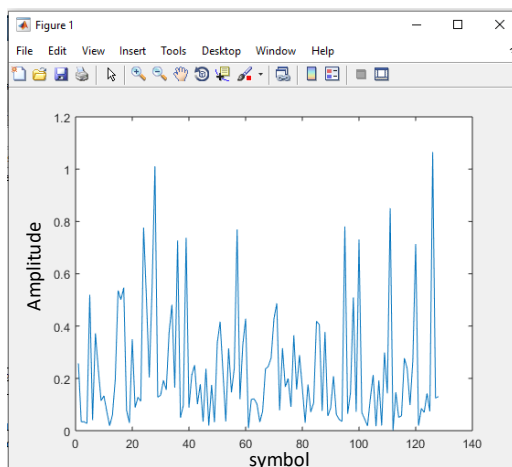


Figure 26 : SER for SF =7 and SNR = -15.

```
Command Window

SNR =

    -15

symbol_errors_rate =

    0.5740

fx >>
```

- SF = 9 (intermediate SF)

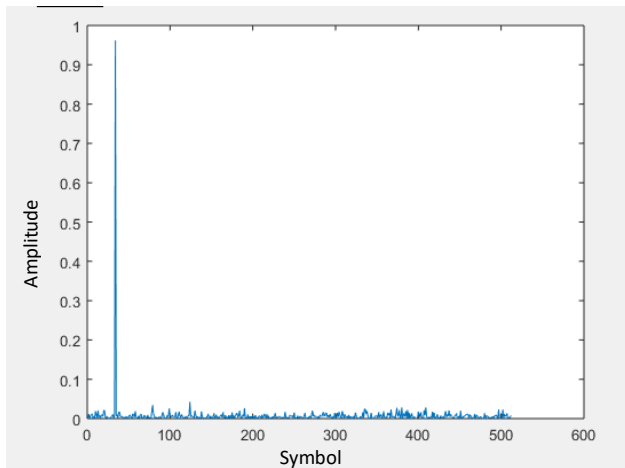


Figure 28 SER for SF =9 and SNR = -5.

```
Command Window
SNR =
    -5

symbol_errors_rate =
     0
```

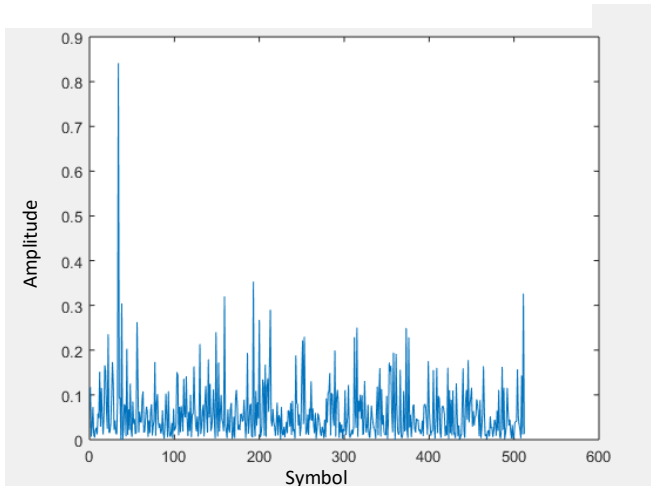


Figure 27 : Figure 27 SER for SF =9 and SNR = -15.

```
Command Window
SNR =
   -15

symbol_errors_rate =
  0.0200
```

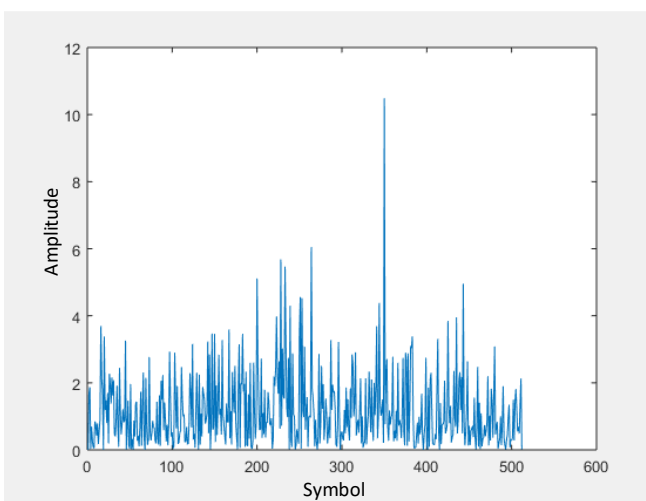
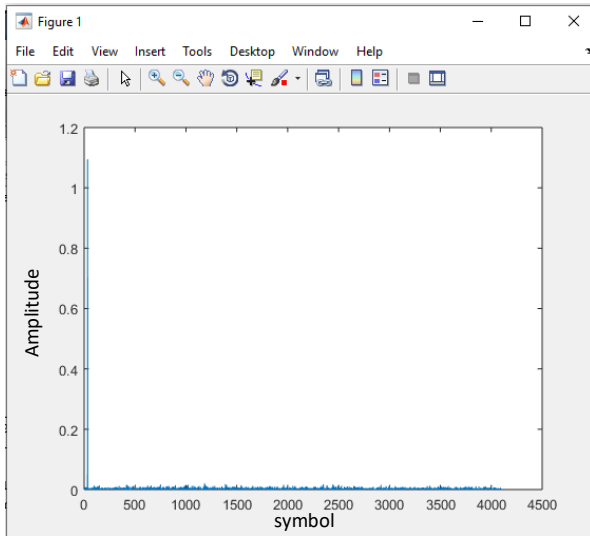


Figure 29 : Figure 27 SER for SF =9 and SNR = -28.

```
Command Window
SNR =
   -28

symbol_errors_rate =
  0.9870
```

- SF = 12 (high SF)



```

Command Window

SNR =

    -10

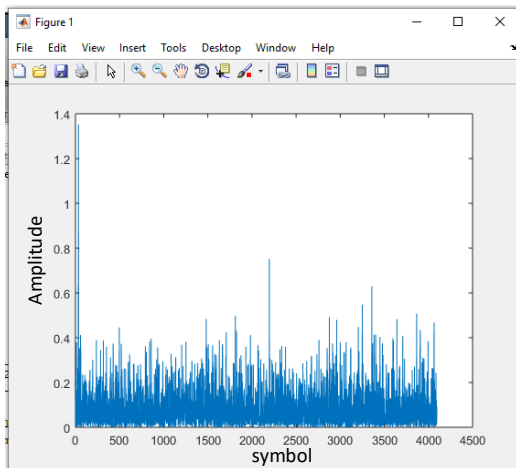
symbol_errors_rate =

     0

fx >> s

```

Figure 30 : Figure 27 SER for SF =12 and SNR = -10.



```

Command Window

SNR =

    -25

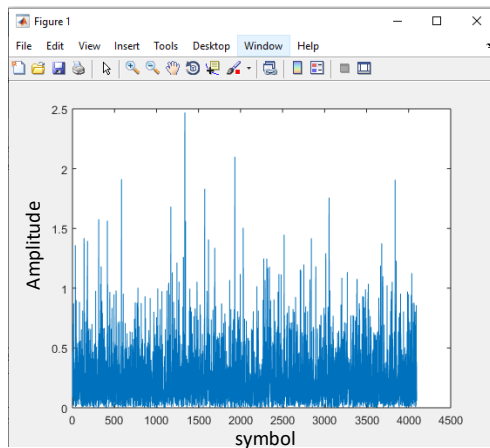
symbol_errors_rate =

    0.1910

fx >> s

```

Figure 31 : Figure 27 SER for SF =9 and SNR = -25.



```

Command Window

SNR =

    -30

symbol_errors_rate =

    0.8700

fx >> s

```

Figure 32 : Figure 27 SER for SF =9 and SNR = -30.

III.4 Simulation Discussion

III.4.1 Impact of SNR on Error Rate

The simulation results clearly demonstrate the relationship between SNR and Error Rate (ER) for different Spreading Factors (SF). As observed from the graph and the table, the Error Rate decreases as the SNR increases, which aligns with the theoretical expectations. Higher SNR indicates a clearer signal with less noise, thereby improving the accuracy of symbol detection and reducing the error rate.

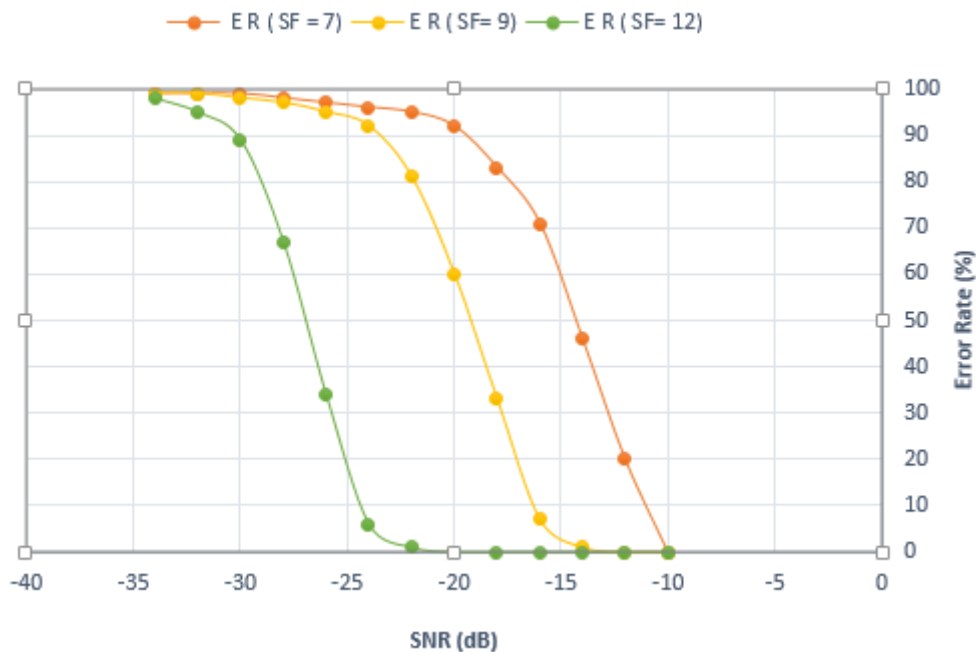


Figure 33 : Impact of SNR on Error Rate.

For SF = 9:

- The error rate remains at 0% up to an SNR of -20 dB, showing more robustness compared to SF = 7.
- However, at lower SNR values, the error rate sharply increases. For instance, at SNR = -22 dB, the error rate jumps to 80%, highlighting a significant sensitivity to noise at lower SNRs.

For SF = 12:

- This spreading factor shows the highest robustness to noise. The error rate remains at 0% for SNR values up to -22 dB.

- It maintains a relatively low error rate even at SNRs as low as -26 dB, where the error rate is 97%.
- The transition to a high error rate occurs more gradually compared to lower spreading factors.

III.4.1.1 Trade-off between Spreading Factor, Range, and Data Rate

The Spreading Factor (SF) in LoRa modulation significantly impacts the range and data rate of communication. Higher SF values result in more extended communication ranges but lower data rates. Conversely, lower SF values provide higher data rates but shorter ranges.

III.4.1.1.1 Higher Spreading Factor (SF = 12)

- Range: Higher SFs enable longer-range communication. This is due to the increased time duration of each chirp symbol, which makes the signal more resilient to noise and interference.
- Data Rate: The trade-off is a lower data rate. Higher SF means that each symbol takes longer to transmit, reducing the overall data throughput.

III.4.1.1.2 Lower Spreading Factor (SF = 7)

- Range: Lower SFs are suitable for shorter-range communication. The shorter chirp symbols are more susceptible to noise, limiting the effective communication range.
- Data Rate: The advantage is a higher data rate. The shorter duration of each chirp symbol allows for more symbols to be transmitted in the same time period, increasing the data throughput.

III.4.1.1.3 Intermediate Spreading Factor (SF = 9)

- Range and Data Rate: This provides a balance between range and data rate. It offers moderate robustness to noise and a reasonable data rate, making it suitable for scenarios where neither extreme range nor maximum data rate is required.

III.5 Simulation Conclusion

The simulation results clearly illustrate the impact of SNR on the performance of LoRa modulation for different Spreading Factors. Higher spreading factors offer better noise resilience and longer communication ranges at the cost of lower data rates. Lower spreading

factors provide higher data rates but are more susceptible to noise and have shorter communication ranges. These trade-offs must be carefully considered when designing LoRa-based communication systems to meet specific application requirements.

In summary, selecting the appropriate SF for a given application depends on the required communication range, acceptable error rate, and necessary data throughput. Understanding the relationship between SNR, SF, and their effects on communication performance is crucial for optimizing LoRa network deployments.

III.6 Designing the Communication System: Component Selection and PCB Layout

In the development of the communication subsystem for an educational CubeSat, the primary focus is on reliable and efficient data transmission between the satellite and ground stations. The system utilizes the SX1280 LoRa transceiver, known for its long-range and low-power capabilities, integrated with an Arduino Nano microcontroller. This setup ensures robust communication while managing power consumption effectively. The payload includes various sensors to monitor environmental conditions and system health.

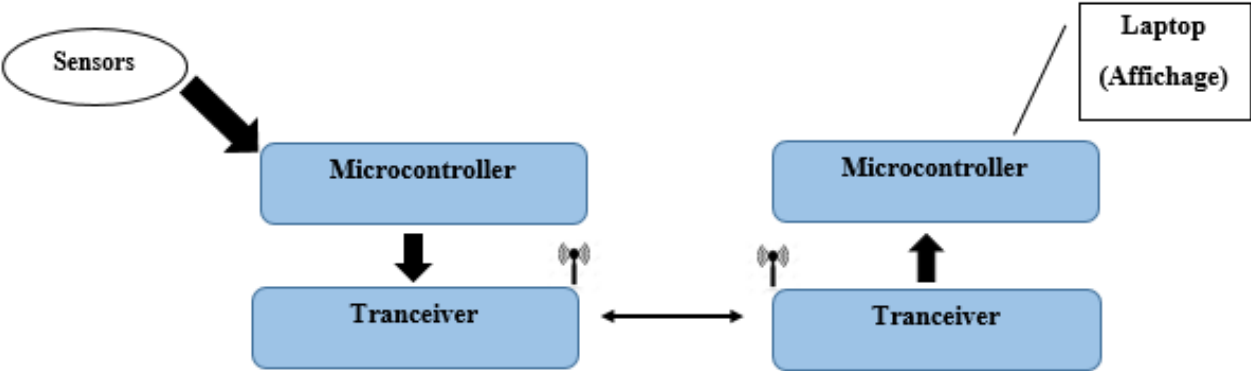


Figure 34 : fundamental communication system for an educational CubeSat.

This diagram illustrates a fundamental communication system for an educational CubeSat. It consists of two main parts: the CubeSat subsystem and the ground station subsystem. The CubeSat collects data from various sensors and transmits it to the ground station for analysis and display.

III.6.1 Component Selection for the Communication System

In this section, we'll discuss about the selected components for our CubeSat's communication system, including the SX1280 LoRa transceiver, Arduino Nano microcontroller, and various sensors.

III.6.1.1 SX1280 Transceiver

The SX1280 transceiver is a high-performance, low-power wireless transceiver designed for use in a variety of applications, including IoT, industrial automation, and consumer electronics. It operates in the 2.4 GHz frequency band and supports a range of modulation schemes, including LoRa [16].

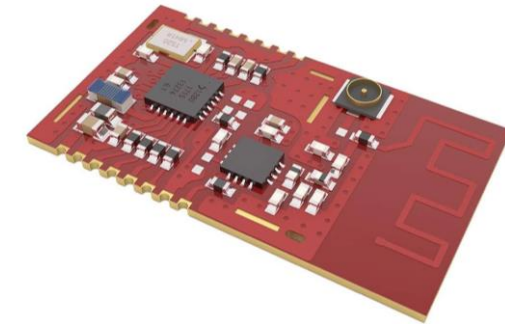


Figure 35 : SX1280 Transceiver [23].

The SX1280 transceiver from Semtech Corporation is a suitable choice for CubeSat communication systems due to its long-range communication capabilities, high sensitivity, and high-efficiency power amplifier. It also has low power consumption, compact size, and programmable bit rate features, making it well-equipped to handle the challenges of transmitting and receiving data over long distances in the harsh space environment [16].

III.6.1.2 Arduino Nano

The Arduino Nano is an excellent choice for the CubeSat communication subsystem due to its small footprint, low power consumption, and flexibility. Its compact size fits well within the constrained space of a CubeSat, and its low power requirements are ideal for battery-powered space applications. The Arduino Nano's compatibility with a wide range of sensors and the SX1280 LoRa transceiver simplifies integration and ensures reliable data transmission. Additionally, the user-friendly Arduino IDE streamlines development and debugging, making it easier to implement and maintain the communication system [25].

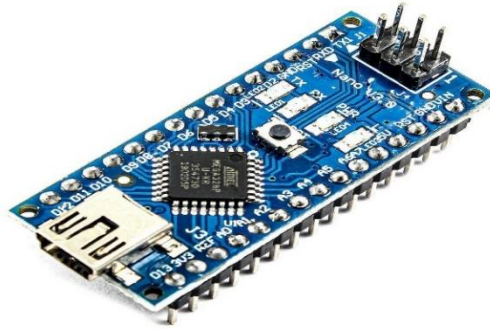


Figure 36 : Arduino Nano module[25].

III.6.1.3 Sensors

This subsystem consists of a variety of sensors that are responsible for acquiring scientific data. The selection and integration of these sensors is a crucial aspect of the CubeSat design process.

III.6.1.3.1 ICM 20948 Module

The ICM-20948 is a high-performance, low-power 9-axis motion tracking device from TDK InvenSense. It integrates a 3-axis gyroscope, a 3-axis accelerometer, and a 3-axis magnetometer, all in a single package [26].

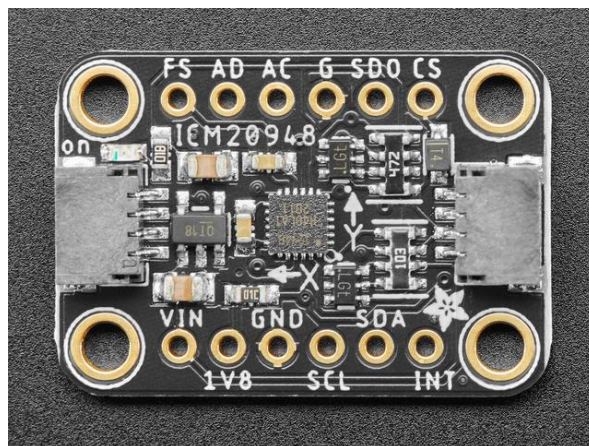


Figure 37 : ICM 20948 Module[26].

The ICM-20948 is a crucial component in CubeSat subsystems, particularly for attitude determination and control, as well as payload monitoring. In the Attitude Determination and Control System (ADCS), it provides real-time orientation data, stabilizes the CubeSat, and assists in precise navigation by tracking the satellite's orientation relative to Earth and celestial bodies. For payload monitoring, the ICM-20948 tracks vibrations and movements, ensuring the payload remains within operational limits

and supports experiments requiring precise orientation and movement tracking. Its low power consumption and high accuracy make it ideal for power-efficient and reliable CubeSat operations [26].

III.6.1.3.2 NEO-6M GPS Module

The NEO-6M is a GPS module from u-blox, renowned for its high performance and accuracy in satellite navigation. It is widely used in various applications requiring reliable and precise positioning data [27].

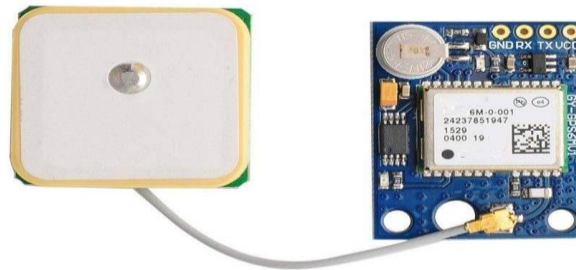


Figure 38 : NEO-6M GPS Module[27].

The NEO-6M GPS module is integral to several CubeSat subsystems, especially for navigation, positioning, and timing functions. It provides precise position data for accurate orbital determination, assists in path planning and ground tracking, and ensures the CubeSat follows its intended orbit. In the Attitude Determination and Control System (ADCS), it helps align the CubeSat's coordinate system with Earth's reference frame and works with sensors like the ICM-20948 to enhance accuracy. The module offers precision timing for synchronized operations and event scheduling, crucial for efficient mission management. Additionally, it facilitates real-time tracking and telemetry by sending position data back to ground stations, aiding in status monitoring and emergency location.

III.6.1.3.3 DHT 11 Module

The DHT11 sensor is a popular digital sensor that measures temperature and humidity. It is commonly used in various applications due to its simplicity, low cost, and ease of integration with microcontrollers and other electronic system [28].

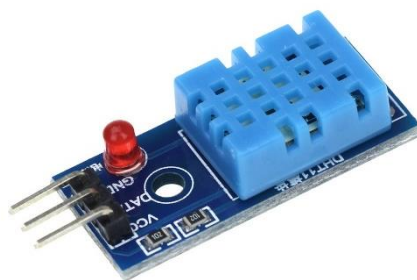


Figure 39 : DHT 11 Module [28].

The DHT11 sensor is used in CubeSats for monitoring internal temperature and humidity, aiding in thermal control, and ensuring the optimal operating conditions of electronic components, all while being low-power, compact, easy to integrate.

III.6.1.4 Antenna

The antenna is a vital component of the cubesat communication subsystem, responsible for both transmitting and receiving signals. The choice of antennas directly impacts the efficiency, range, and reliability of the communication link between the cubesat and ground stations.

- **Transmission : Dipole Antenna (2.4 GHz)**

For transmitting data from our cubesat to the ground station, we utilize a dipole antenna operating at 2.4 GHz. The dipole antenna is chosen for its simplicity, omnidirectional radiation pattern, and efficient performance at the specified frequency. This allows for effective transmission of data across various orientations of the satellite in space.



Figure 40 : 2.4 GHz dipole antenna with SMA connector [32].

- **Reception: WiFi Yagi Antenna (2.4 GHz)**

For receiving data from the ground station, we employ a WiFi Yagi antenna, also operating at 2.4 GHz. The Yagi antenna is selected due to its high sensitivity and directional capabilities, which significantly enhance the range and reliability of the communication link. This directional focus allows the cubesat to receive weaker signals from the ground station, ensuring robust communication even over longer distances.

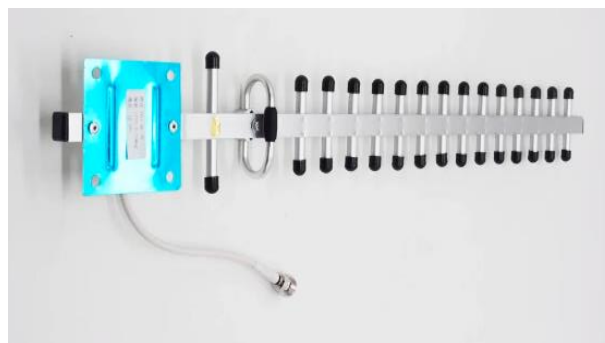


Figure 41 : WiFi Yagi Antenna (2.4 GHz)[33].

Here's a comparison table between the Yagi antenna from and the TP-Link dipole antenna [32] [33].

Table 3 : comparison table between the Yagi antenna from and the TP-Link dipole antenna [32] [33].

Feature	Yagi Antenna	Tp-link dipole antenna (TL-ANT2409CL)
Frequency Range	2.4 Ghz	2.4 Ghz
Gain	16 dBi	9 dBi
Radiation Pattern	Directional	Omnidirectional
Connector	SMA male	SMA male
Impedence	50 Ohms	50 Ohms
VSWR(voltage standing wave ratio)	≤ 1.5	≤ 1.92
Polarization	Vertical	Vertical
Weight	250g (approx.)	168g
Application	Long-Range , directional communication	Medium-range , omnidirectional communication

III.7 CubeSat Communication System: Schematic and PCB Blueprint

Below, we present the design schematic for the CubeSat's communication system. This schematic shows how all the parts are connected and work together. We used the EasyEDA online design tool.

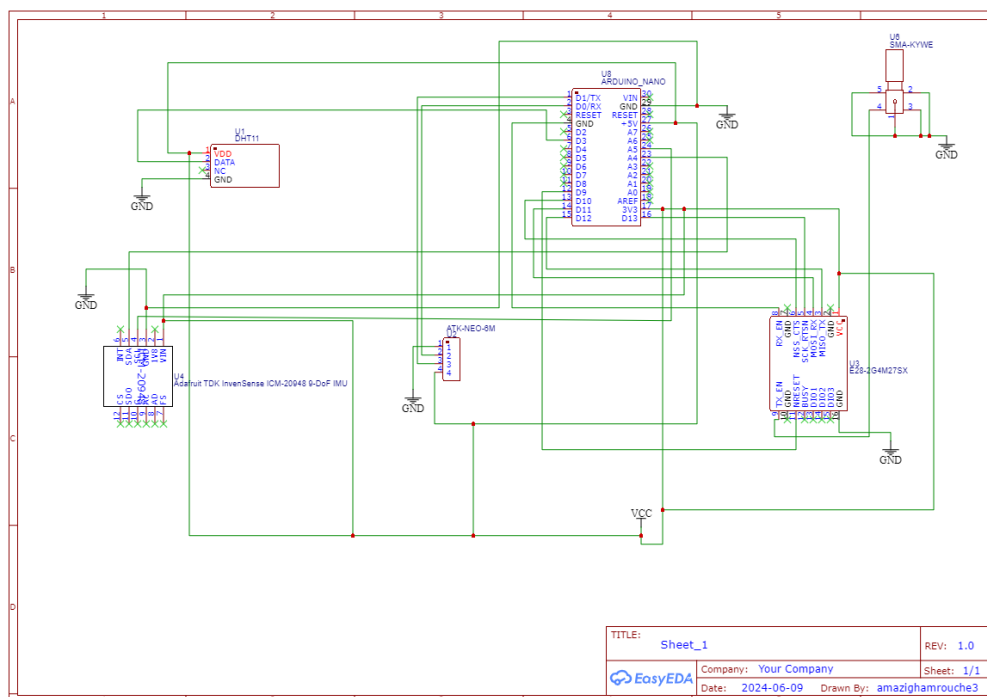


Figure 42 : Design schematic for the emission part .

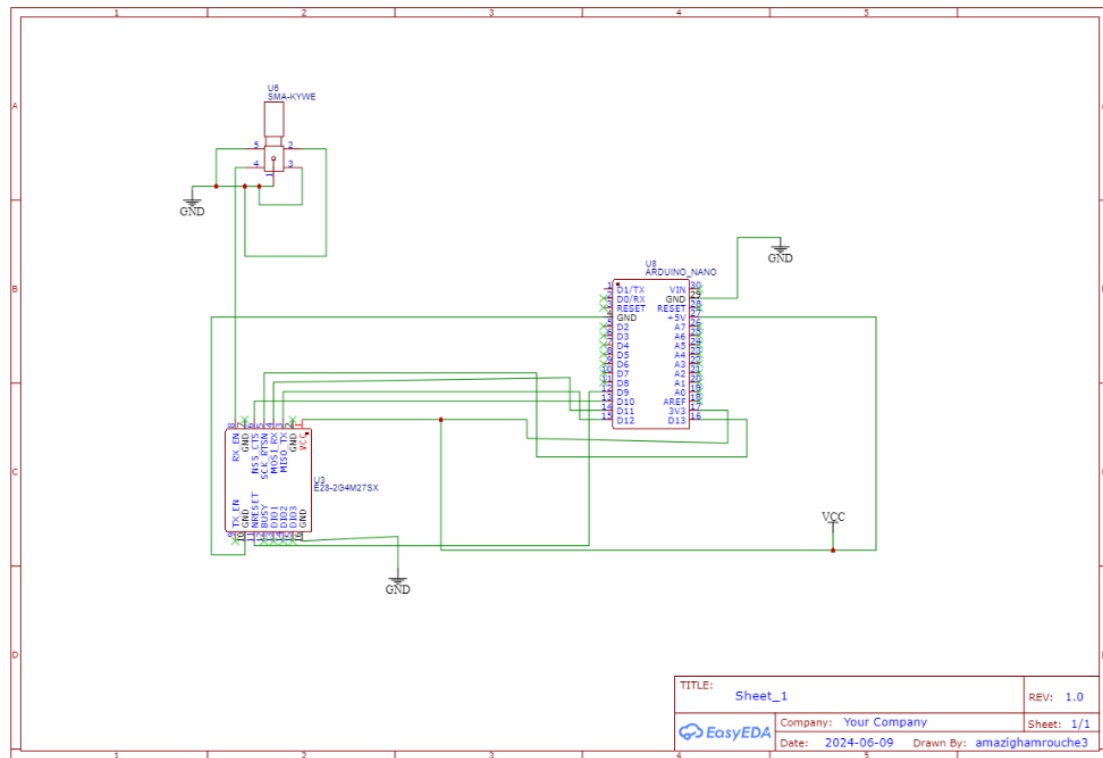


Figure 43 : Design schematic for the reception part.

The provided schematics offer a detailed view of the CubeSat communication system, comprising both emission and reception subsystems. The emission system is equipped with several sensors: the DHT11 sensor measures temperature and humidity, the IMU (Inertial Measurement Unit) monitors the CubeSat's orientation and motion, and the GPS module provides precise positioning data. These sensors are all managed by an Arduino Nano microcontroller, which collects and processes the sensor data. Once processed, the data is transmitted via a transceiver module, enabling the CubeSat to send information to ground stations or other satellites.

On the other hand, the reception system is designed to handle incoming signals. It includes an SMA connector that attaches to an external antenna, which captures RF signals. These signals are then fed into a transceiver module that converts them into a format suitable for processing by the Arduino Nano microcontroller. The Arduino Nano in the reception system demodulates and processes the received signals, converting them back into useful data.

Both schematics emphasize the interconnectedness of these components, showcasing how the CubeSat effectively manages data collection, transmission, and reception. The emission system ensures comprehensive environmental monitoring and data transmission,

while the reception system guarantees reliable signal capture and processing. This detailed arrangement highlights the sophisticated communication capabilities of the CubeSat, with each component playing a crucial role in maintaining its functionality and efficiency in space.

III.8 PCB design

This section represents the design of the PCB board for the emission and reception modules

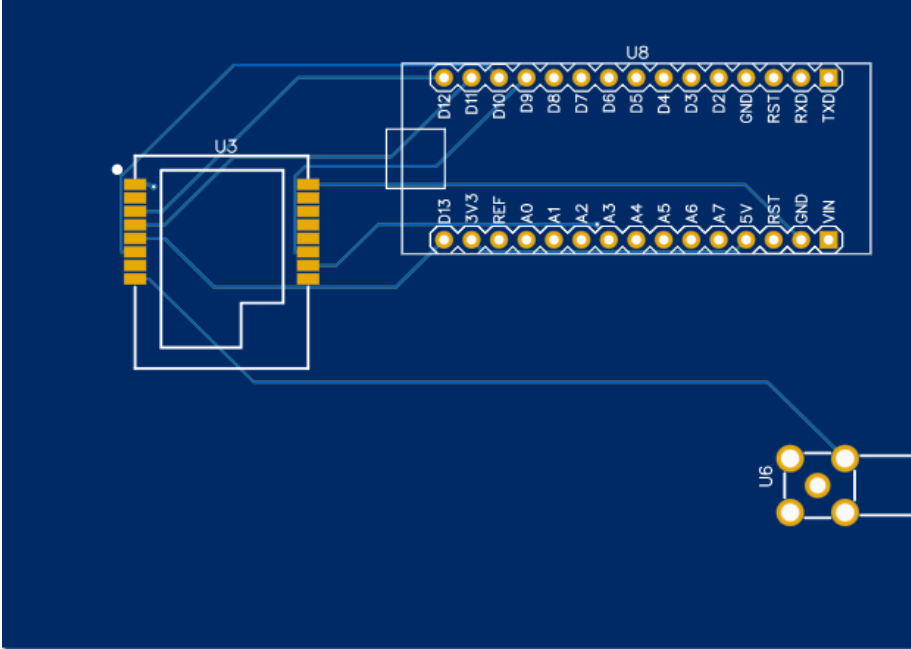


Figure 45 PCB Design schematic for the Reception part

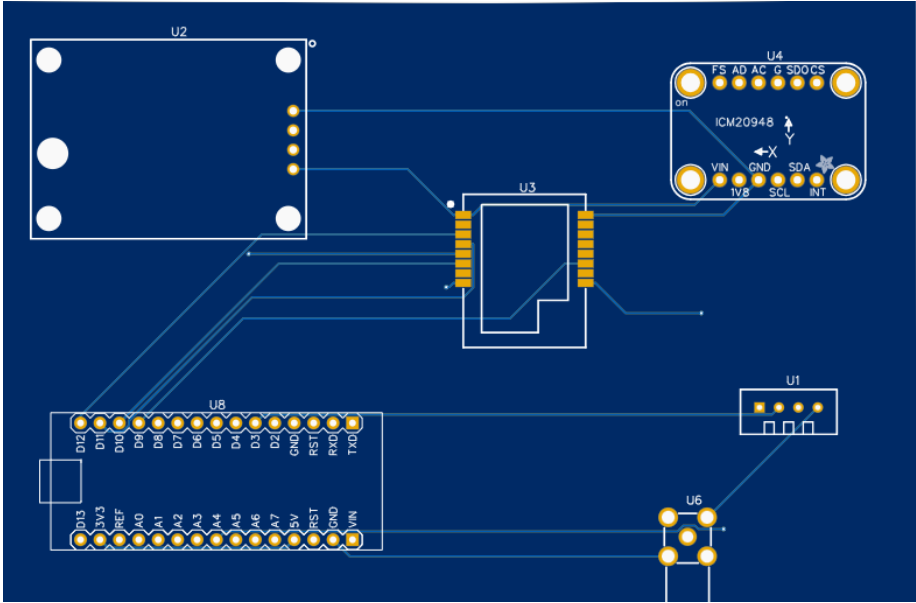


Figure 44 PCB Design schematic for the emission part

III.9 Conclusion

In this chapter, we have thoroughly examined the simulation and performance evaluation of LoRa communication in CubeSat systems. Our analysis began with a detailed simulation of LoRa signals, exploring the impact of noise and various spreading factors (SF) on signal integrity and communication efficiency. We demonstrated how different noise levels and SF settings can significantly affect the performance of LoRa communication, providing insights into optimizing these parameters for reliable data transmission in the space environment. Additionally, we discussed the critical component selection for this system, including the transceiver, microcontroller, different sensors, and antenna, emphasizing their roles and specifications to ensure optimal performance. Furthermore, we schematized the communication system, illustrating the integration of key components and their interactions. This groundwork culminated in the detailed PCB design for both the emission and reception modules, ensuring efficient and robust communication capabilities for the CubeSat. This comprehensive approach not only highlights the challenges and solutions in implementing LoRa communication in CubeSat systems but also lays a solid foundation for future advancements and practical applications in this domain.

General Conclusion

Our master's thesis presented a comprehensive exploration and design initiative for a CubeSat communication subsystem, focusing particularly on the implementation of LoRa modulation. The study began with an in-depth examination of the CubeSat communication system, laying out the critical requirements and challenges associated with satellite communication

Thesis topics focused on the intricacies of LoRa modulation. We thoroughly investigated its properties, performance indicators, and appropriateness for CubeSat communication requirements. This investigation was both theoretical and practical, including the use of a simulation model to test the efficacy and dependability of LoRa modulation in a CubeSat scenario.

We next continued on to the design phase, with an emphasis on hardware implementation. The SX1280 transceiver was chosen as the foundation of our communication subsystem because to its extensive features and compatibility with LoRa modulation. We thoroughly constructed the PCB and developed detailed schematics for the system to ensure that all components were properly adjusted for best performance.

Unfortunately, time restrictions prevented the communication subsystem from being fully realized. Regardless, the foundations presented in this thesis provides a solid platform for future research. Future initiatives can build on this foundation to complete the reality of the communication subsystem by leveraging and enhancing the schematics and PCB designs created here. This thesis not only illustrates the possibility of employing LoRa modulation for CubeSat communication, but it also provides a significant resource for future research in this subject.

References

- [1] <https://www.spacefoundation.org/2023/07/25/the-space-report-2023-q2/>.
- [2] Dr. –Ing. Toshinori Kuwahara , "Introduction to Small Satellite " ,Tohoku University Department of Aerospace Engineering ,KiboCUBE Academy ,lecture 07 , (2023).
- [3] Wood, D., & Weigel, A. (2012). Charting the evolution of satellite programs in developing countries – The Space Technology Ladder. ScienceDirect, 26(1), 123-138. DOI: 10.1016/j.actaastro.2011.06.008.
- [4] "Nanosatellites: A New Era in Space Exploration" by J. Smith (2020).
- [5] "The Future of Space Exploration: Nanosatellites and Beyond" by M. Johnson (2022).
- [6] "Nanosatellites: A Guide to Design, Development, and Launch" by T. Lee (2021).
- [7] natalia cebrián herrera , (2014) . a case study on the communications subsystem for cubesat . universitat politècnica.
- [8] Dr. Engineering. Masahiko Yamazaki , "Introduction to CubeSat Payload System", Nihon University Department of Aerospace Engineering, KiboCUBE Academy ,lecture 18 , (2022).
- [9] https://ntrs.nasa.gov/api/citations/20210016644/downloads/ccaaw_2021_final.pdf.
- [10] Lin, Shu, and Daniel J. Costello Jr. Error Control Coding: Fundamentals and Applications. Prentice Hall, (2004).book.
- [11] <http://connections-qj.org/article/semtech-an120022-lora-modulation-basics..>
- [12] <https://wirelesspi.com/understanding-lora-phy-long-range-physical-layer/>.
- [13] Dong-Hoon, Kim Eun-kyu Lee and Jibum Kim , Experiencing LoRa Network establishment on a smart energy campus testbed , Sustainability journal , (2019).page 05.
- [14] <https://blog.ttulka.com/lora-spreading-factor-explained/>.

- [15] <https://www.rfwireless-world.com/Terminology/What-is-difference-between-Chip-and-Chirp-in-LoRaWAN.html>.
- [16] <https://www.digikey.be/en/products/base-product/semtech-corporation/600/SX1280/336165>.
- [17] "A Comparative Study of FSK and LoRa for Low-Power Wide-Area Networks" IEEE Communications Magazine, vol. 55, no. 9, 2017.
- [18] Petäjäjärvi, J., Mikhaylov, K., Pettissalo, M., Janhunen, J., & Inatti, J. (2017). Performance of a low-power wide-area network based on LoRa technology: Doppler robustness, scalability, and coverage. International Journal of Distributed Sensor Networks, 13(3), doi:10.1177/1550147717699412.
- [19] D. R. Lorenz, A. J. Witzgall, S. L. Smith, "Software-Defined Radio for CubeSat Applications," IEEE Aerospace Conference, Big Sky, MT, USA, 2017, pp. 1-9.
- [20] S. Thampi, S. S. Sreelal, V. Rajakumar, S. Gurubaran, S. Baghel, P. Muralikrishna, K. G. Jaleel, N. Vineeth, A. G. Das, S. Umopathy, K. Joshi, P. Sreekumar, and A. K. Patra, "Design and realization of a CubeSat for ionospheric scattering observations," April 2018.
- [21] <https://www.crowdsupply.com/lime-micro/limesdr-mini>.
- [22] <https://greatscottgadgets.com/hackrf/>.
- [23] <https://www.ebay.com/itm/385527220729>
- [24] Sklar, B. (2001). Digital Communications: Fundamentals and Applications. Prentice Hall.
- [25] <https://electropeak.com/nano-arduino-board>
- [26] <https://learn.adafruit.com/adafruit-tdk-invensense-icm-20948-9-dof-imu/overview>
- [27] https://www.u-blox.com/sites/default/files/products/documents/NEO-6_DataSheet_%28GPS.G6-HW-09005%29.pdf..
- [28] <https://fr.sz-kuongshun.com/uno/uno-sensor/dht11-temperature-and-humidity-sensor-module-with.html>
- [29] <https://www.isispace.nl/product/cubesat-antenna-system-1u-3u/>

[30] 10.1109/SmartIoT49966.2020.00048

[31] <https://doi.org/10.3390/s21082774>

[32] <https://www.tp-link.com/au/business-networking/antenna-and-accessory/tl-ant2409c1/>

[33] <https://www.aliexpress.com/i/2251832693306454.html?gatewayAdapt=4itemAdapt>